

Proximal Learning for Individualized Treatment Regimes Under Unmeasured Confounding

Zhengling Qi*, Rui Miao†, Xiaoke Zhang†

Abstract

Data-driven individualized decision making has recently received increasing research interests. Most existing methods rely on the assumption of no unmeasured confounding, which unfortunately cannot be ensured in practice especially in observational studies. Motivated by the recently proposed proximal causal inference, we develop several proximal learning approaches to estimating optimal individualized treatment regimes (ITRs) in the presence of unmeasured confounding. In particular, we establish several identification results for different classes of ITRs, exhibiting the trade-off between the risk of making untestable assumptions and the value function improvement in decision making. Based on these results, we propose several classification-based approaches to finding a variety of restricted in-class optimal ITRs and develop their theoretical properties. The appealing numerical performance of our proposed methods is demonstrated via an extensive simulation study and a real data application.

Keywords: Proximal causal inference, Endogeneity, Treatment regime identification, Double robustness

*Department of Decision Sciences, The George Washington University

†Department of Statistics, The George Washington University

1 Introduction

In recent years, data-driven individualized decision making has received increasing research interests in various scientific fields. In precision medicine, researchers leverage biomedical data to discover better treatment regimes for heterogeneous patients [e.g., [Rashid et al., 2020](#)]. In mobile health research, due to the recent advances in smart devices and sensing technology, real time information is collected and used to learn the most effective interventions for patients in order to promote healthy behaviors [e.g., [Klasnja et al., 2015](#)]. In robotics, tremendous simulated data are generated to train robots for making optimal decisions to complete different human tasks [e.g., [Kober et al., 2013](#)]. In operations management, learning the optimal resource allocation based on current conditions, logistics and costs, etc, is necessary to improve the efficiency of operations [e.g., [Seong et al., 2006](#)]. Apparently a common goal of all these problems above is to find the optimal individualized treatment regime (ITR) that can optimize the outcome of each individual.

Many statistical and machine learning methods have been developed for the optimal ITR learning. For example, [Qian and Murphy \[2011\]](#) proposed to learn the optimal ITR by first fitting a high-dimensional regression model for the conditional expectation of outcome given treatment and covariates [so-called Q-function, [Watkins and Dayan, 1992](#)] and then assigning an treatment to each individual with the largest Q-function value. In the binary treatment setting, this method is equivalent to estimating the conditional average treatment effect. Methods of such type are usually referred to as model-based methods [e.g., [Zhao et al., 2009](#), [Shi et al., 2018](#)]. Alternatively, direct methods have been proposed in the literature, which directly maximize the value function (defined in [\(1\)](#) below) over a class of ITRs. For example, [Zhao et al. \[2012\]](#) applied inverse probability weighting (IPW) to estimate the value function for each ITR, and then leveraged modern classification techniques to learn the optimal one. Along this line of research, various extensions have been proposed, such as [Zhao et al. \[2014\]](#) for censored outcomes, [Chen et al. \[2016\]](#) for ordinal outcomes and [Wang et al. \[2018\]](#) for quantile optimal treatment regimes among others. To alleviate potential model misspecifications of the Q-function or propensity score, especially in observational studies, augmented IPW has been used to estimate the value function so that the estimated value function enjoys the doubly robust property [e.g., [Zhang et al., 2012](#), [Dudík et al., 2011](#)]. Later on, borrowed from semiparametric

statistics [Bickel, 1982, Chernozhukov et al., 2018], cross-fitting techniques have been incorporated to further improve the efficiency of the doubly robust optimal ITR estimator [Athey and Wager, 2021, Zhao et al., 2019]. See Kosorok and Laber [2019] and references therein for a review.

A majority of the existing methods in the literature rely on a key assumption that there is no unmeasured confounding so that the Q-function or value function can be identified nonparametrically using observed data. However, in practice, it is difficult to guarantee or verify that assumption, especially in observational studies or randomized trials with non-compliance. Therefore practitioners often try to remove confounding effects and thus identify optimal ITRs by collecting and adjusting for as many variables as possible. While this strategy might be the best we have to adopt in practice, it is generally elusive. To address this limitation, the instrumental variable (IV) has been used in the literature to provide a valid and rigorous way of learning the optimal ITR in the presence of unmeasured confounding. For example, Cui and Tchetgen Tchetgen [2020] and Qiu et al. [2020] independently established similar identification results on the value function using IVs and proposed different learning methods, one for deterministic ITRs and the other for stochastic ITRs. While these two methods are useful, especially in randomized trials with non-compliance, their restriction that the IV must be binary may limit their applicability. Han [2019] and Pu and Zhang [2020] relaxed the assumption of exactly identifying the value function and provided robustness in estimating ITRs by considering the partial identification under the IV setting. Although partial identification can still provide valuable treatment regimes to policy makers, their methods may only lead to sub-optimal ITRs.

In this paper, we propose an alternative approach to estimating optimal ITRs under endogeneity. Our work is built upon the recently developed *proximal causal inference* by Miao and Tchetgen Tchetgen [2018] and Tchetgen Tchetgen et al. [2020], which enables the causal effect identification based on observed data when the assumption of no unmeasured confounding fails to hold. The salient idea behind proximal causal inference is to identify the causal effect in terms of either treatment-inducing confounding proxies or outcome-inducing confounding proxies, which connects the existing causal effect identification results under the frameworks of IV and negative controls. The applicability of proximal causal inference is very promising since the existence of such proxies is reasonable in some applications [see Miao and Tchetgen Tchetgen, 2018, Tchetgen Tchetgen et al., 2020, for examples] and moreover their data types are not restrictive, compared with some IV approaches discussed in

the previous paragraph. More recently, the semiparametric efficiency problem under this framework has also been studied [Cui et al., 2020]. By adapting the idea of proximal causal inference, we establish identification results on different classes of ITRs under various scenarios and accordingly propose several classification-based approaches to estimating the restricted in-class optimal ITRs.

The contribution of this paper is threefold. First, we establish several new identification results on various classes of ITRs with unmeasured confounding in terms of treatment-inducing and/or outcome-inducing confounding proxies. All these results can show the trade-off between the risk of making untestable assumptions and the potential gain of value function in decision making. Note that since covariates are involved in ITRs, our identification results are focused on the conditional treatment effect, which are different from those for the average treatment effect as in the proximal causal inference literature. Second, based on these identification results, we propose several classification-based learning approaches to estimating optimal ITRs. For nuisance functions involved in these approaches, we apply the min-max learning method in Dikkala et al. [2020] to estimate them nonparametrically, generalizing the parametric method by Cui et al. [2020]. Similar methods have also been used in Kallus et al. [2021] and Ghassami et al. [2021], which were posted on arxiv.org very recently, and are independent works from this paper. Under one specific setting where the causal effect can be identified via either a treatment-inducing confounding bridge function or an outcome-inducing confounding bridge function (see Section 3 below), we develop a doubly robust optimal ITR learning approach and adopt the idea of cross-fitting to improve its efficiency (see Section 4.3 below). Third, we establish theoretical guarantees for the proposed doubly robust proximal learning approaches. Specifically, we provide a finite sample bound for the value function difference between the optimal ITR and our estimated in-class optimal ITR. The bound can be decomposed into four parts: an irreducible error due to unmeasured confounding, an approximation error due to the restricted treatment regime class, and two estimation errors. The theoretical results for other proposed methods can be similarly derived.

The rest of our paper is organized as follows. In Section 2, we briefly introduce the framework of learning optimal ITRs without unmeasured confounding. Then we discuss how to nonparametrically identify different classes of treatment regimes under the proximal causal inference framework in Section 3. In Section 4, we develop several corresponding proximal learning methods under various identification conditions. The related theoretical results are presented in Section 5. In Sections 6 and

7 respectively, we show the superior performance of our methods via extensive simulation studies and one real data application. Conclusions and future directions along this line of research are discussed in Section 8.

2 Optimal ITR Without Unmeasured Confounding

In this section, we give a brief introduction to finding the optimal ITR without unmeasured confounding. Let A be a binary treatment which takes values in the treatment space $\mathcal{A} = \{-1, 1\}$ and let $Y(1)$ and $Y(-1)$ be the potential outcome if $A = 1$ and -1 respectively. In practice only $Y = Y(1)\mathbb{I}(A = 1) + Y(-1)\mathbb{I}(A = -1)$ is observable, where $\mathbb{I}(\bullet)$ denotes an indicator function, but $Y(1)$ and $Y(-1)$ are not both observable. Denote X as the observed p -dimensional covariate that belongs to a covariate space $\mathcal{X} \subset \mathbb{R}^p$. Without loss of generality, we assume that a larger outcome Y is more preferred.

Since a larger Y is more preferred, typically the optimal ITR is defined as the treatment assignment which maximizes the expected value of the potential outcome. Explicitly, let \mathcal{D} be the class of all ITRs where each ITR $d \in \mathcal{D}$ is a measurable function mapping from the covariate space \mathcal{X} into the treatment space \mathcal{A} . Then the potential outcome under any $d \in \mathcal{D}$ can be defined by

$$Y(d) = Y(1)\mathbb{I}(d(X) = 1) + Y(-1)\mathbb{I}(d(X) = -1),$$

and the value function of d [Manski, 2004, Qian and Murphy, 2011] is defined by

$$V(d) \triangleq \mathbb{E}\{Y(d)\}. \tag{1}$$

Under the following three standard assumptions in the counterfactual framework [Robins, 1986]: (i) $Y(1), Y(-1) \perp\!\!\!\perp A \mid X$ where $\perp\!\!\!\perp$ represents independence; (ii) $\Pr(A = a \mid X) > 0$ for every $a \in \mathcal{A}$ almost surely; (iii) $Y = Y(A)$, we can nonparametrically identify the value function $V(d)$ by

$$V(d) = \mathbb{E}\left\{\frac{Y\mathbb{I}(A = d(X))}{\Pr(A \mid X)}\right\}. \tag{2}$$

Then by maximizing $V(d)$ in (2) over \mathcal{D} , the *global* optimal ITR can be shown as

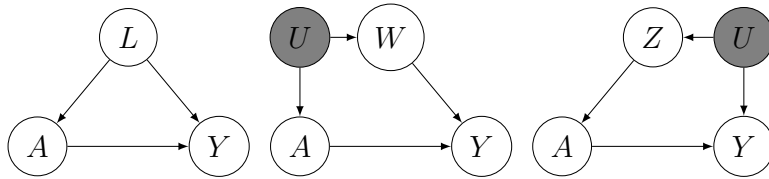
$$d^*(X) \triangleq \text{sign} \{ \mathbb{E}(Y | X, A = 1) - \mathbb{E}(Y | X, A = -1) \},$$

almost surely. See Qian and Murphy [2011] and Zhao et al. [2012] for more details. Lastly, we remark that there is no difference in finding optimal ITRs if we use other coding schemes for A such as $1/0$.

3 Optimal ITR With Unmeasured Confounding

Hereafter we no longer assume no unmeasured confounding, i.e., $Y(1), Y(-1) \perp\!\!\!\perp A | X$ may not hold. When there exist unmeasured confounders U that affect both treatment A and outcome Y , unless we make proper assumptions, we are not able to identify the value function based on observed data as in (2) or further to find optimal ITRs [Pearl, 2009]. Inspired by the proximal casual inference recently proposed by Miao and Tchetgen Tchetgen [2018] and Tchetgen Tchetgen et al. [2020], we adapt this idea to the optimal ITR learning in the presence of unmeasured confounding.

Following Tchetgen Tchetgen et al. [2020], suppose that we can decompose measured covariates X into three types $X = (L, W, Z)$, where L affect both A and Y , W are *outcome-inducing confounding proxies* that are only related to treatment A through (L, U) , and Z are *treatment-inducing confounding proxies* that are only related to outcome Y through (L, U) . Here we adopt the same terminologies for Z and W as those in Tchetgen Tchetgen et al. [2020], but they are also called negative control exposure and negative control outcome respectively [e.g., Miao and Tchetgen Tchetgen, 2018]. Figure 1 provides an illustration of their relationships with A and Y respectively. In general, such decomposition does not guarantee the identifiability of the causal effect. For example, as shown in Figure 2 where L, W, Z and $U = (U_1, U_2, U_3)$ coexist, the path $A-U_2-U_3-U_1-Y$ prevents us from identifying the causal effect of A on Y . However, there also exists scenarios where the no unmeasured confounding assumption still holds and thus the causal effect of A on Y can be identified. See Figure 1 (b)-(c) and Figure 1 (d) of Tchetgen Tchetgen et al. [2020] for examples. Therefore, given the decomposition $X = (L, W, Z)$, it is possible to relax the no unmeasured confounding assumption and still identify the causal effect of A on Y .



(a) measured covariates L ; (b) outcome proxies; (c) treatment proxies;

Figure 1: Directed acyclic graph representations when no unmeasured confounding holds.

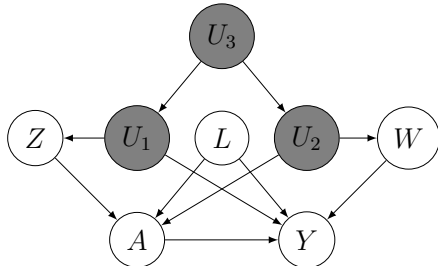


Figure 2: An unidentifiable causal effect when L, W, Z and $U = (U_1, U_2, U_3)$ coexist.

Compared with average treatment effect estimation, we need to further take the class of treatment regimes into consideration in optimal ITR learning since an ITR depends on observed covariates, so this may further limit our ability of identifying the value function. In the following, we present several basic assumptions and then show different value function identification results under various additional assumptions. Denote the spaces of L, U, W , and Z as $\mathcal{L}, \mathcal{U}, \mathcal{W}$ and \mathcal{Z} respectively.

3.1 Basic Assumptions

Below we list several basic assumptions for value function identification with unmeasured confounding. For more details, see [Tchetgen Tchetgen et al. \[2020\]](#).

Assumption 1 (Consistency). $Y = Y(A)$ almost surely.

Assumption 2 (Positivity). $\Pr(A = a \mid U, L) > 0$ for every $a \in \mathcal{A}$ almost surely.

Assumption 3 (Outcome-inducing confounding proxies). $W(a, z) = W$ for all $a \in \mathcal{A}$ and $z \in \mathcal{Z}$ almost surely.

Assumption 4 (Treatment-inducing confounding proxies). $Y(a, z) = Y(a)$ for all $a \in \mathcal{A}$ and $z \in \mathcal{Z}$ almost surely.

Assumption 5 (Latent exchangeability). $(Z, A) \perp (Y(a), W) \mid (U, L)$ for every $a \in \mathcal{A}$.

Assumptions 1 and 2 are standard in the literature of causal inference with no unmeasured confounding. Assumption 1 links the potential outcome with the observed outcome while Assumption 2 states that each treatment has a chance of being assigned.

Assumption 3 essentially states that A and Z do not have a causal effect on W while Assumption 4 indicates that there is no direct causal effect of Z on Y except intervening on A . Assumption 5 indicates that by adjusting for (U, L) , one is able to jointly identify the causal effect of (Z, A) on Y and W , which holds in principle as U is not observed. Notice that by Assumption 5, \mathcal{D} becomes the class of all ITRs mapping from (L, U) into \mathcal{A} , and the *global* optimal ITR within \mathcal{D} becomes

$$d^*(L, U) = \text{sign} \{ \mathbb{E}(Y \mid L, U, A = 1) - \mathbb{E}(Y \mid L, U, A = -1) \},$$

almost surely, which is similar to its counterpart in Section 2. A directed acyclic graph (DAG) of Assumptions 3–5 is depicted in Figure 3.

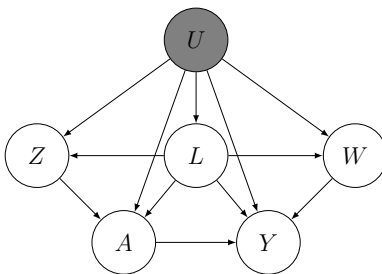


Figure 3: A causal DAG as a representation of Assumptions 3–5.

Under Assumptions 1–5 and a few additional assumptions listed below, we establish several value function identifications under unmeasured confounding.

3.2 Optimal ITR via Outcome Confounding Bridge

Here we propose the first value function identification without assuming no unmeasured confounding. This requires the following technical assumptions used by Miao et al. [2018] to identify the population average treatment effect in the presence of unmeasured confounding.

Assumption 6 (Completeness). (a) For any $a \in \mathcal{A}, l \in \mathcal{L}$ and measurable function g over \mathcal{U} , if $\mathbb{E}\{g(U) \mid Z, A = a, L = l\} = 0$ almost surely, then $g(U) = 0$ almost surely.

(b) For any $a \in \mathcal{A}, l \in \mathcal{L}$ and measurable function g over \mathcal{Z} , if $\mathbb{E}\{g(Z) \mid W, A = a, L = l\} = 0$ almost surely, then $g(Z) = 0$ almost surely.

Assumption 7 (Outcome Confounding Bridge). There exists an outcome confounding bridge function h_0 over $(\mathcal{W}, \mathcal{A}, \mathcal{L})$ such that

$$\mathbb{E}(Y \mid Z, A, L) = \mathbb{E}\{h_0(W, A, L) \mid Z, A, L\}, \quad (3)$$

almost surely.

Assumption 6 is commonly seen in the theory of mathematical statistics and can be satisfied by a wide range of parametric or semiparametric models such as those for exponential families [Newey and Powell, 2003]. For more examples including nonparametric models, we refer readers to D’Haultfoeuille [2011] and Chen et al. [2014]. Assumption 6 (a) essentially requires that the variability of U can be accounted for by Z and Assumption 6 (b) can be similarly interpreted. Assumption 6 does not require specific types of confounders, which thus provides a broad application.

Assumption 7 basically states that there exists a solution to the so-called inverse problem in (3), which is a linear integral equation of the first kind [Kress et al., 1989]. Assumption 6 (b), together with some regularity conditions given by Miao et al. [2018], can imply the existence of such h_0 satisfying (3). For more details and practical examples where these assumptions are satisfied, we refer readers to Miao et al. [2018], Shi et al. [2020] and Miao and Tchetgen Tchetgen [2018].

Based on the outcome confounding bridge function h_0 , we develop a nonparametric identification result for ITRs, which is similar to that by Miao and Tchetgen Tchetgen [2018] on the average treatment effect.

Theorem 3.1. *Let \mathcal{D}_1 be the class of ITRs that map from $(\mathcal{L}, \mathcal{Z})$ into \mathcal{A} . Under Assumptions 1-5, 6(a) and 7, for any $d_1 \in \mathcal{D}_1$, the value function $V(d_1)$ can be nonparametrically identified by*

$$V(d_1) = \mathbb{E} \{h_0(W, d_1(L, Z), L)\}. \quad (4)$$

Then the restricted in-class optimal ITR within \mathcal{D}_1 , defined as $d_1^ \in \arg \max_{d_1 \in \mathcal{D}_1} V(d_1)$, can be identified by*

$$d_1^*(L, Z) = \text{sign} [\mathbb{E} \{h_0(W, 1, L) \mid L, Z\} - \mathbb{E} \{h_0(W, -1, L) \mid L, Z\}], \quad (5)$$

almost surely.

The proof of Theorem 3.1 is given in Supplementary Material S2. Theorem 3.1 indicates that value function is identifiable over \mathcal{D}_1 in spite of the existence of unmeasured confounders. Due to the use of the outcome confounding bridge function h_0 , we can only identify the value function over a restricted class of ITRs \mathcal{D}_1 instead of \mathcal{D} . Notice that since W is used as outcome-inducing proxies, it is not considered as a decision variable for the optimal treatment regime. We would rather investigate how the covariates Z and L could affect the outcome Y (or the proximal outcome W).

The form of d_1^* in (5) shows that the optimal ITR in \mathcal{D}_1 incorporates the effect of treatment-inducing proxies Z on Y unless $\mathbb{E} \{h_0(W, 1, L) \mid L, Z\} - \mathbb{E} \{h_0(W, -1, L) \mid L, Z\}$ is independent of Z . This may be reasonable since Z may contain some useful information of U , which can help improve the value function. See simulation studies in Section 6.3. Obviously $V(d_1^*) \leq V(d^*)$, but due to unmeasured confounding, $V(d_1^*)$ is the best we can obtain within \mathcal{D}_1 under the assumptions in Theorem 3.1. To illustrate how to obtain d_1^* via h_0 , a concrete example is provided in Supplementary Material S1.

3.3 Optimal ITR via Treatment Confounding Bridge

To identify the value function and thus obtain the optimal ITR within a certain class of treatment regimes based on observed data, Assumptions 6 and 7 are not the only assumptions we can use in the presence of unmeasured confounding. In this section, we consider the following alternative assumptions, which were originally used by Cui et al. [2020] to identify the average treatment effect.

Assumption 8 (Completeness). (a) For any $a \in \mathcal{A}, l \in \mathcal{L}$ and measurable function g over \mathcal{U} , if

$$\mathbb{E}\{g(U) \mid W, A = a, L = l\} = 0 \text{ almost surely, then } g(U) = 0 \text{ almost surely.}$$

(b) For any $a \in \mathcal{A}, l \in \mathcal{L}$ and measurable function g over \mathcal{W} , if $\mathbb{E}\{g(W) \mid Z, A = a, L = l\} = 0$

almost surely, then $g(W) = 0$ almost surely.

Assumption 9 (Treatment Confounding Bridge). There exists a treatment confounding bridge function q_0 over $(\mathcal{Z}, \mathcal{A}, \mathcal{L})$ such that

$$\frac{1}{\Pr(A = a \mid W, L)} = \mathbb{E}\{q_0(Z, A, L) \mid W, A = a, L\}, \quad (6)$$

almost surely.

Assumptions 8 and 9 play a similar role of Assumptions 6 and 7. In particular, Assumption 9 establishes a link between Z and A and Equation (6) is also a linear integral equation of the first kind. The existence of such q_0 satisfying (9) can be guaranteed by Assumption 8 (b) combined with some regularity conditions given in Cui et al. [2020].

Similar to Theorem 3.1, we can instead use the treatment confounding bridge function to nonparametrically identify the value function over a certain class of ITRs.

Theorem 3.2. Let \mathcal{D}_2 be the class of ITRs that map from $(\mathcal{L}, \mathcal{W})$ into \mathcal{A} . Under Assumptions 1-5, 8(a) and 9, the value function $V(d_2)$ can be nonparametrically identified by

$$V(d_2) = \mathbb{E}\{Yq_0(Z, A, L)\mathbb{I}(d_2(L, W) = A)\}, \quad (7)$$

Then the restricted optimal ITR within \mathcal{D}_2 , defined as $d_2^* \in \arg \max_{d_2 \in \mathcal{D}_2} V(d_2)$, can be identified by

$$d_2^*(L, W) = \text{sign}[\mathbb{E}\{Y\mathbb{I}(A = 1)q_0(Z, 1, L) \mid L, W\} - \mathbb{E}\{Y\mathbb{I}(A = -1)q_0(Z, -1, L) \mid L, W\}], \quad (8)$$

almost surely.

The proof of Theorem 3.2 is given in Supplementary Material S2. Similar to the discussion after Theorem 3.1, Theorem 3.2 shows that the value function is identifiable over \mathcal{D}_2 in terms of the

treatment confounding bridge q_0 despite unmeasured confounding. Such a result in Theorem 3.2 can be useful in identifying a restricted optimal ITR when W should and Z should not be included in a treatment policy, as kindly pointed out by one reviewer. For instance, in the time series example given in Miao and Tchetgen Tchetgen [2018], when there is no feedback effects, future exposure can serve as Z and past outcomes can be W . Therefore it is reasonable to consider W as a decision variable for the treatment regime while Z should not be.

3.4 Optimal ITR based on Both Confounding Bridges

In Sections 3.2 and 3.3 above, we establish the results for the value function and optimal ITR identification in terms of the outcome confounding bridge and treatment confounding bridge respectively. A natural question arises here: Is it possible to obtain a broader identification result if both confounding bridges coexist? The answer is affirmative.

If Assumptions 1–5, 6 (a), 7, 8 (a), 9, by Theorems 3.1 and 3.2, it is clear that $V(d_4)$ can be identified for any $d_4 \in \mathcal{D}_1 \cup \mathcal{D}_2$ by

$$V(d_4) = \mathbb{I}(d_4 \in \mathcal{D}_1) \mathbb{E} \{h_0(W, d_4(L, Z), L)\} \\ + \mathbb{I}(d_4 \in \mathcal{D}_2) \mathbb{E} \{Y_{q_0}(Z, A, L) \mathbb{I}(d_4(L, W) = A)\}.$$

Then the restricted optimal ITR in $\mathcal{D}_1 \cup \mathcal{D}_2$ is defined as

$$d_4^* \in \arg \max_{d_4 \in \mathcal{D}_1 \cup \mathcal{D}_2} V(d_4). \tag{9}$$

Even under these assumptions above, we are still unable to estimate the value function $V(d)$ based on observed data over $d \in \tilde{\mathcal{D}}$, the class of all ITRs mapping from (L, W, Z) into \mathcal{A} , since $\mathbb{E} \{Y(a) \mid L, W, Z\}$ for any $a \in \mathcal{A}$ is not identifiable nonparametrically due to unmeasured confounding. It is unknown whether there exists a sufficient and necessary condition to identify the conditional average treatment effect given observed covariates when there exists unmeasured confounding.

To conclude this section, we provide Table 1 that summarizes the identification results we have developed and their corresponding assumptions. Discussions and practical suggestions on these results

can be found at the end of Section 4.

Table 1: A summary of optimal ITR identification results.

Assumptions	ITR Class	Restricted Optimal ITR
1-5, 6 (a) and 7	$\mathcal{D}_1 : (\mathcal{L}, \mathcal{Z}) \rightarrow \mathcal{A}$	d_1^* in (5) through h_0
1-5, 8 (a) and 9	$\mathcal{D}_2 : (\mathcal{L}, \mathcal{W}) \rightarrow \mathcal{A}$	d_2^* in (8) through q_0
1-5, 6 (a), 7, 8 (a) and 9	$\mathcal{D}_1 \cup \mathcal{D}_2$	d_4^* in (9) through q_0 or h_0

4 Proximal Policy Learning

In this section, we discuss optimal ITR estimations based on observed n independent and identically distributed samples $\{(L_i, Z_i, W_i, A_i, Y_i) : i = 1, \dots, n\}$. In Section 4.1 we will first propose the estimation methods for confounding bridge functions h_0 and q_0 defined in Assumptions 7 and 9 respectively. Then in Section 4.2, based on the estimates of h_0 and q_0 , we will propose several classification-based approaches to estimating d_1^* , d_2^* , and d_4^* under their corresponding assumptions respectively. In addition, in Section 4.3, when Assumptions 1-5, 6 (a), 7, 8 (a) and 9 hold, we propose a doubly robust and an augmented inverse probability weighted (AIPW)-type classification-based method for estimating the optimal ITR with a class of ITRs, which are all measurable functions mapping from \mathcal{L} into \mathcal{A} . We denote this class by \mathcal{D}_3 and the corresponding restricted optimal ITR by d_3^* .

In the remainder of this paper, we let Assumptions 6 (b) and 8 (b) always hold so that h_0 and q_0 can be uniquely identified respectively by completeness.

4.1 Estimation of Confounding Bridge Functions

Here we introduce nonparametric estimations of outcome and treatment confounding bridge functions h_0 and q_0 defined in Assumptions 7 and 9 respectively.

Estimating h_0 : Equation (3) in Assumption 7 is equivalent to

$$\mathbb{E}\{Y - h_0(W, A, L) \mid Z, A, L\} = 0, \quad (10)$$

which is known as the instrumental variable model or conditional moment restriction model and has been well studied in econometrics and statistics [e.g., Chamberlain, 1992, Newey and Powell, 2003, Ai and Chen, 2003, Blundell et al., 2007, Chen, 2007, Chen and Pouzo, 2012].

Here we adopt the min-max estimation method by Dikkala et al. [2020] to estimate h_0 nonparametrically as follows:

$$\hat{h}_0 = \arg \min_{h \in \mathcal{H}} \sup_{f \in \mathcal{F}} \left[\frac{1}{n} \sum_{i=1}^n \{Y_i - h(W_i, A_i, L_i)\} f(Z_i, A_i, L_i) - \lambda_{1,n} \|f\|_{\mathcal{F}}^2 - \|f\|_{2,n}^2 \right] + \lambda_{2,n} \|h\|_{\mathcal{H}}^2, \quad (11)$$

where $\lambda_{1,n} > 0$ and $\lambda_{2,n} > 0$ are tuning parameters, $\|\bullet\|_{2,n}$ is the empirical ℓ^2 norm, i.e., $\|f\|_{2,n} = \sqrt{n^{-1} \sum_{i=1}^n f^2(Z_i, A_i, L_i)}$, and \mathcal{H} and \mathcal{F} are some functional classes, e.g., reproducing kernel Hilbert spaces (RKHS), with their corresponding norms $\|\bullet\|_{\mathcal{F}}$ and $\|\bullet\|_{\mathcal{H}}$ respectively.

The rationale behind (11) is the following population version of min-max optimization problem when $\lambda_{1,n}, \lambda_{2,n} \rightarrow 0$ as $n \rightarrow \infty$:

$$\min_{h \in \mathcal{H}} \sup_{f \in \mathcal{F}} \left(\mathbb{E} [\{Y - h(W, A, L)\} f(Z, A, L)] - \mathbb{E} \{f^2(Z, A, L)\} \right). \quad (12)$$

If $2^{-1} \mathbb{E} \{h_0(W, A, L) - h(W, A, L) \mid Z, A, L\} \in \mathcal{F}$ for every $h \in \mathcal{H}$, then the optimization (12) above is equivalent to

$$\min_{h \in \mathcal{H}} \mathbb{E} \left([\mathbb{E} \{Y - h(W, A, L) \mid Z, A, L\}]^2 \right).$$

If we further assume $h_0 \in \mathcal{H}$, then h_0 is the unique global minimizer of (12). Hence the min-max formulation (11) is reasonable.

Estimating q_0 : Equation (6) in Assumption 9 indicates that for every $a \in \mathcal{A}$,

$$\mathbb{E} [\{\mathbb{I}(A = a)q_0(Z, A, L) - 1\} \mid W, L] = 0.$$

Similar to (11), we estimate q_0 by the following min-max optimization: For each $a \in \mathcal{A}$,

$$\hat{q}_0(\bullet, a, \bullet) = \arg \min_{q \in \mathcal{Q}} \left(\sup_{g \in \mathcal{G}} \left[\frac{1}{n} \sum_{i=1}^n \{\mathbb{I}(A_i = a)q(Z_i, a, L_i) - 1\} g(W_i, L_i) - \mu_{1,n} \|g\|_{\mathcal{G}}^2 - \|g\|_{2,n}^2 \right] + \mu_{2,n} \|q\|_{\mathcal{Q}}^2 \right), \quad (13)$$

where $\mu_{1,n} > 0$ and $\mu_{2,n} > 0$ are tuning parameters, and \mathcal{Q} and \mathcal{G} are functional classes, with their corresponding norms $\|\bullet\|_{\mathcal{Q}}$ and $\|\bullet\|_{\mathcal{G}}$.

Generally one may use any functional class for \mathcal{H} and \mathcal{F} in (11) and for \mathcal{Q} and \mathcal{G} in (13). If they are all specified as RKHS, due to the representer theorem, both \hat{h}_0 and \hat{q}_0 have finite-dimensional representations which can facilitate fast computations. See Supplementary Material S3. for computational details.

4.2 Outcome and Treatment Proximal Learning

With estimated h_0 and q_0 , we propose to estimate optimal ITRs using classification-based approaches which are similar to those of Zhao et al. [2012] and Zhang et al. [2012] under no unmeasured confounding. We develop estimation procedures for d_1^* and d_2^* respectively based on different assumptions and identification results in Section 3.

Outcome Proximal Learning of d_1^* : By (5) under the assumptions in Theorem 3.1, finding d_1^* is equivalent to minimizing the following classification error

$$\mathbb{E}[\{h_0(W, 1, L) - h_0(W, -1, L)\} \mathbb{I}(d_1(L, Z) \neq 1)],$$

over all $d_1 \in \mathcal{D}_1$. Since each $d_1 \in \mathcal{D}_1$ can be written as $d_1(L, Z) = \text{sign}\{r_1(L, Z)\}$ for some measurable function r_1 defined on $(\mathcal{L}, \mathcal{Z})$, we can rewrite $\mathbb{I}(d_1(L, Z) \neq 1) = \mathbb{I}(r_1(L, Z) < 0)$ where $\text{sign}(0) \triangleq 1$. Then the optimization problem above becomes

$$\min_{r_1} \mathbb{E}[\{h_0(W, 1, L) - h_0(W, -1, L)\} \mathbb{I}(r_1(L, Z) < 0)].$$

Given observed data and \hat{h}_0 , we consider its empirical version as

$$\min_{r_1} \frac{1}{n} \sum_{i=1}^n \hat{\Delta}(W_i, L_i) \mathbb{I}(r_1(L_i, Z_i) < 0),$$

where $\hat{\Delta}(W, L) = \hat{h}_0(W, 1, L) - \hat{h}_0(W, -1, L)$, or equivalently

$$\min_{r_1} \frac{1}{n} \sum_{i=1}^n \left| \hat{\Delta}(W_i, L_i) \right| \mathbb{I} \left(\text{sign} \left(\hat{\Delta}(W_i, L_i) \right) r_1(L_i, Z_i) < 0 \right). \quad (14)$$

The equivalence above motivates us to use a convex surrogate function to replace the indicator function since all weights $|\hat{\Delta}(W_i, L_i)|$ are non-negative. Similar to [Zhao et al. \[2012\]](#) and [Zhao et al. \[2019\]](#), we adopt the hinge loss $\phi(t) = \max(1 - t, 0)$ and consider $r_1 \in \mathcal{R}_1$, a pre-specified class of functions defined on $(\mathcal{L}, \mathcal{Z})$, e.g., a RKHS, to obtain the estimated optimal ITR by $\hat{d}_1^* = \text{sign}(\hat{r}_1)$ where

$$\hat{r}_1 \in \arg \min_{r_1 \in \mathcal{R}_1} \left\{ \frac{1}{n} \sum_{i=1}^n \left| \hat{\Delta}(W_i, L_i) \right| \phi \left(\text{sign} \left(\hat{\Delta}(W_i, L_i) \right) r_1(L_i, Z_i) \right) + \rho_{1,n} \|r_1\|_{\mathcal{R}_1}^2 \right\}, \quad (15)$$

$\|\bullet\|_{\mathcal{R}_1}$ is the norm of \mathcal{R}_1 and $\rho_{1,n} > 0$ is a tuning parameter. The optimization in (15) is convex and thus can be solved efficiently. See details in Algorithm 1 of Supplementary Material S3.

Treatment Proximal Learning of d_2^* : Similar to learning d_1^* , by (8) and the assumptions of Theorem 3.2 and with \hat{q}_0 , we propose to first find \hat{r}_2 , the solution to the following minimization

$$\min_{r_2 \in \mathcal{R}_2} \left\{ \frac{1}{n} \sum_{i=1}^n \left| Y_i \hat{q}_0(Z_i, A_i, L_i) \right| \phi \left(A_i \text{sign} \left(Y_i \hat{q}_0(Z_i, A_i, L_i) \right) r_2(L_i, W_i) \right) + \rho_{2,n} \|r_2\|_{\mathcal{R}_2}^2 \right\}, \quad (16)$$

where $\|\bullet\|_{\mathcal{R}_2}$ is the norm of a pre-specified class of functions \mathcal{R}_2 defined on $(\mathcal{L}, \mathcal{W})$, e.g., a RKHS, and then obtain the estimated optimal ITR by $\hat{d}_2^* = \text{sign}(\hat{r}_2)$. See details in Algorithm 4 of Supplementary Material S3.

Maximum Proximal Learning of d_4^* : By (9) and Assumptions 1-9, obtaining d_4^* is equivalent to solving

$$\max \left\{ \max_{d_1 \in \mathcal{D}_1} V(d_1), \max_{d_2 \in \mathcal{D}_2} V(d_2) \right\}. \quad (17)$$

Therefore, we combine the learning approaches in (15) and (16) and use a cross-validation procedure to find the estimated optimal ITR \hat{d}_4^* , i.e., the better decision rule between \hat{d}_1^* and \hat{d}_2^* . See details in Algorithm 5 of Supplementary Material S3.

4.3 Doubly Robust Proximal Learning

In practice, one may be interested in treatment policies only based on L (e.g., when outcome and treatment proxies are not observed in the future decision making). Let \mathcal{D}_3 be the class of all ITRs that map from \mathcal{L} into \mathcal{A} and $d_3^* \in \arg \max_{d_3 \in \mathcal{D}_3} V(d_3)$. Here we propose an estimation of d_3^* . Since d_3^* is the optimal ITR within \mathcal{D}_3 defined on \mathcal{L} only, the value function $V(d_3)$ can be identified by either h_0 or q_0 , for any $d_3 \in \mathcal{D}_3$ if all Assumptions 1–9 are satisfied. Leveraging this, in the following we develop a doubly robust estimator for $V(d_3)$ over \mathcal{D}_3 , which provides a protection against the potential model misspecification of h_0 or q_0 , in the sense that as long as either h_0 and q_0 is modelled correctly, the doubly robust estimator is consistent. This is motivated by the efficient influence function of $V(d_3)$ given below.

Theorem 4.1. *Under Assumptions 1–9 and some regularity conditions given in Theorem 3.1 of Cui et al. [2020], the efficient influence function of $V(d_3)$ is*

$$\mathbb{I}(A = d_3(L))q_0(Z, A, L) \{Y - h_0(W, A, L)\} + h_0(W, d_3(L), L) - V(d_3), \quad (18)$$

for any given $d_3 \in \mathcal{D}_3$.

The proof is similar to that of Cui et al. [2020] and is thus omitted. Denote

$$C_1(Y, L, W, Z; h_0, q_0) \triangleq \mathbb{I}(A = 1)q_0(Z, 1, L) \{Y - h_0(W, 1, L)\} + h_0(W, 1, L), \quad (19)$$

$$C_{-1}(Y, L, W, Z; h_0, q_0) \triangleq \mathbb{I}(A = -1)q_0(Z, -1, L) \{Y - h_0(W, -1, L)\} + h_0(W, -1, L). \quad (20)$$

Then based on (18), we can estimate $V(d_3)$ for each $d_3 \in \mathcal{D}_3$ by

$$\begin{aligned} \hat{V}^{DR}(d_3) = & \frac{1}{n} \sum_{i=1}^n \left\{ C_1(Y_i, L_i, W_i, Z_i; \hat{h}_0, \hat{q}_0) \mathbb{I}(d_3(L_i) = 1) \right. \\ & \left. + C_{-1}(Y_i, L_i, W_i, Z_i; \hat{h}_0, \hat{q}_0) \mathbb{I}(d_3(L_i) = -1) \right\}. \end{aligned} \quad (21)$$

The $\hat{V}^{DR}(d_3)$ above enjoys the doubly robust property in the sense that $\hat{V}^{DR}(d_3)$ is consistent to $V(d_3)$ for each $d_3 \in \mathcal{D}_3$ as long as one of the nuisance functions q_0 and h_0 is modeled correctly, not

necessarily both.

Then following similar arguments in Section 4.2, we can estimate d_3^* by first obtaining the decision function \hat{r}^{DR} via

$$\begin{aligned} \hat{r}_3^{DR} \in \arg \min_{r \in \mathcal{R}_3} & \left[\frac{1}{n} \sum_{i=1}^n \left\{ \left| C_1(Y_i, L_i, W_i, Z_i; \hat{h}_0, \hat{q}_0) \right| \phi \left(\text{sign} \left(C_1(Y_i, L_i, W_i, Z_i; \hat{h}_0, \hat{q}_0) \right) r(L_i) \right) \right. \right. \\ & \left. \left. + \left| C_{-1}(Y_i, L_i, W_i, Z_i; \hat{h}_0, \hat{q}_0) \right| \phi \left(-\text{sign} \left(C_{-1}(Y_i, L_i, W_i, Z_i; \hat{h}_0, \hat{q}_0) \right) r(L_i) \right) \right\} + \rho_{4,n} \|r\|_{\mathcal{R}_3}^2 \right], \end{aligned} \quad (22)$$

where \mathcal{R}_3 is a class of functions defined on \mathcal{L} with norm $\|\bullet\|_{\mathcal{R}_3}$ and $\rho_{4,n} > 0$ is a tuning parameter. Then the estimated optimal ITR is $\hat{d}_3^{DR} = \text{sign}(\hat{r}_3^{DR})$.

In practice, we apply the cross-fitting technique [Bickel, 1982, Chernozhukov et al., 2018] to remove the dependence between the nuisance function estimates \hat{h}_0 and \hat{q}_0 , and resulting estimated optimal ITRs, so that the efficiency of the learning procedure can be proved under less restrictive conditions on each of these nuisance functions, e.g., without imposing Donsker conditions on nuisance function estimations, although one needs to estimate two nuisance functions. See Chernozhukov et al. [2018] and Athey and Wager [2021] for more details.

To implement the cross-fitting algorithm, we randomly split data into K folds and apply the following procedure: first use the k -th fold, $k = 1, \dots, K$, to obtain $\hat{h}_0^{(k)}$ and $\hat{q}_0^{(k)}$, the estimates of h_0 and q_0 respectively; then obtain the decision function by solving (22) based on $\hat{h}_0^{(k)}$ and $\hat{q}_0^{(k)}$ using all data with the k -th fold excluded; lastly, aggregate these K decision rules as our final estimated optimal ITR. See details in Algorithm 6 in Supplementary Material S3. We denote the resulting decision function by \hat{r}_3^{DR} and corresponding estimated optimal ITRs by $\hat{d}_3^{DR} = \text{sign}(\hat{r}_3^{DR})$ with some abuse of notations.

Finally, we provide Table 2 which summarizes each optimal ITR learning and its corresponding assumptions. Note that compared with Table 1, we need additional Assumptions 6 (b) and 8 (b) so that q_0 and h_0 can be uniquely identified by completeness, respectively.

Remark 1. *Table 2 reveals two important trade-offs for proximal ITR learning. The first trade-off is between improving the value function in decision making and imposing more untestable assumptions. For example, the comparison between \hat{d}_4^* and \hat{d}_1^* shows that although we can identify a much larger class*

of ITRs and thus a potentially higher value function for \hat{d}_4^* than \hat{d}_1^* , the maximum proximal learning \hat{d}_4^* requires extra assumptions on the existence of a treatment confounding bridge. Conversely, fewer assumptions are needed for learning d_1^* , which is thus more reliable, but its optimal value function might be more conservative. The second trade-off is between the estimation robustness, and improving the value function in the decision making. For example, in order to estimate d_4^* accurately for obtaining a better value function, we require that both nuisance functions can be estimated consistently. However, if one is willing to consider a smaller class, e.g., \mathcal{D}_3 , one can estimate d_3^* consistently as long as one of these two nuisance functions is estimated consistently, therefore trading off the gain in value function for robustness.

Remark 2. Due to the aforementioned two trade-offs, we suggest practitioners consider a conservative way of choosing the final optimal ITR estimate. Since identifying \mathcal{D}_1 and \mathcal{D}_2 require fewer assumptions than other scenarios, one should trust more on the optimal ITRs learned from the outcome proximal learning or treatment proximal learning, compared with the other two methods. For example, to determine if there is a subgroup that can potentially benefit from a new treatment compared with the standard care, one may recommend the new treatment if both of these two optimal ITR estimates agree. In general, one can also recommend treatments for patients when most of the estimated optimal ITRs agree, to achieve conservativeness, robustness and the gain in improving the value function hopefully in the same time. This ensemble approach is applied in the real data application in Section 7.

Table 2: A summary of the proposed proximal learning methods for optimal ITRs.

Assumptions	ITR Class	Proximal Learning	Estimated Optimal ITR
1-5, 6 (a), 7 and 8 (b)	\mathcal{D}_1	Outcome proximal learning (15)	\hat{d}_1^*
1-5, 6 (b), 8 (a), and 9	\mathcal{D}_2	Treatment proximal learning (16)	\hat{d}_2^*
1- 9	\mathcal{D}_3	Doubly robust proximal learning (22)	\hat{d}_3^{DR}
1- 9	$\mathcal{D}_1 \cup \mathcal{D}_2$	Maximum proximal learning (17)	\hat{d}_4^*

5 Theoretical Results

In this section, we provide theoretical properties of our proposed methods, specifically the finite sample excess risk bound for each of the proposed optimal ITR estimator. For brevity, here we only provide

the results for the doubly robust estimator \hat{d}_3^{DR} , but similar results can be obtained for the other estimators.

We first show the doubly robust property of $\hat{V}^{DR}(d_3)$ in (21) for any $d_3 \in \mathcal{D}_3$.

Proposition 5.1. *Under Assumptions 1-9, if either \hat{h}_0 can consistently estimate h_0 in the sup-norm or \hat{q}_0 can consistently estimate q_0 in the sup-norm, then $\hat{V}^{DR}(d_3)$ is a consistent estimator of $V(d_3)$ for any $d_3 \in \mathcal{D}_3$.*

The proof is given in Supplementary Material S2. Next we show Fisher consistency, that is, it is appropriate to replace the indicator function in \hat{V}^{DR} with the hinge loss as in (22) to obtain \hat{r}_3^{DR} and $\hat{d}_3^{DR} = \text{sign}(\hat{r}_3^{DR})$ accordingly. Define the hinge loss based ϕ -risk by

$$R_\phi(r) = \mathbb{E} \{ |C_1| \phi(\text{sign}(C_1)r(L)) + |C_{-1}| \phi(\text{sign}(C_{-1})r(L)) \}, \quad (23)$$

where C_1 and C_{-1} denote $C_1(Y, L, W, Z; h_0, q_0)$ and $C_{-1}(Y, L, W, Z; h_0, q_0)$ respectively for the ease of presentation. Let $r^* \in \arg \min_r R_\phi(r)$. Then we have the following proposition.

Proposition 5.2. *Under Assumptions 1-9, $d_3^*(L) = \text{sign}(r^*(L))$.*

The proof of Proposition 5.2 is omitted since it can be proved by following similar arguments in the proof of Proposition 3.1 of Zhao et al. [2019]. Proposition 5.2 essentially states that replacing the indicator function by the hinge loss function does not change the goal of finding the optimal ITR.

In addition to Fisher consistency, we can further link the original value function with ϕ -risk as follows.

Proposition 5.3. *Under Assumptions 1-9, $V(d_3^*) - V(d) \leq R_\phi(r) - R_\phi(r^*)$ for any $d = \text{sign}(r(L))$.*

The proof of Proposition 5.3 is omitted due to the same reason as that of Proposition 5.2. Proposition 5.3 implies that the value function difference between the optimal ITR and any other ITR can be bounded by their ϕ -risk difference. Therefore the convergence rate of the value function of \hat{d}_3^{DR} can be bounded by the convergence rate of the ϕ -risk of our estimated decision function \hat{r}_3^{DR} .

To establish the finite sample excess risk bound for \hat{d}_3^{DR} , we make the following technical assumptions in addition to Assumptions 1-9.

Assumption 10. *There exists a constant $C_1 > 0$ such that $\max\{|Y|, \|h_0\|_\infty, \|q_0\|_\infty\} \leq C_1$.*

Assumption 11. *There exist constants $A > 0$ and $v > 0$ such that $\sup_Q N(\mathcal{R}_3, Q, \varepsilon \|F\|_{Q,2}) \leq (A/\varepsilon)^v$ for all $0 < \varepsilon \leq 1$, where $N(\mathcal{R}_3, Q, \varepsilon \|F\|_{Q,2})$ denotes the covering number of the space \mathcal{R}_3 , F is the envelope function of \mathcal{R}_3 , $\|\bullet\|_{Q,2}$ denotes the ℓ_2 -norm under some finitely discrete probability measure Q on (L, \mathcal{L}) , and the supremum is taken over all such probability measures.*

Assumption 12. *The nuisance function estimators $\hat{h}_0^{(k)}$ and $\hat{q}_0^{(k)}$ obtained from the k -th fold of the data in the cross-fitting algorithm in Section 4.3 satisfy that there exist constants $\alpha > 0$ and $\beta > 0$ such that $\left\|h_0(W, a, L) - \hat{h}_0^{(k)}(W, a, L)\right\|_{P,2}^2 = O(n^{-2\alpha})$ and $\left\|q_0(Z, a, L) - \hat{q}_0^{(k)}(Z, a, L)\right\|_{P,2}^2 = O(n^{-2\beta})$ uniformly for all $a \in \mathcal{A}$ and $1 \leq k \leq K$, where P is the underlying probability measure associated with (L, W, Z, A, Y) . In addition, $\max\{\|\hat{q}_0\|_\infty, \|\hat{h}_0\|_\infty\} \leq C_2$ for a constant $C_2 > 0$.*

Assumption 10 requires that the outcome Y is bounded, which is commonly assumed in the literature [e.g., Zhao et al., 2012, Zhou et al., 2017]. Assumption 10 also requires h_0 and q_0 to be both uniformly bounded. Similar conditions on nuisance functions have also been used under the no unmeasured confounding setting [e.g., Zhao et al., 2019]. Assumption 11 essentially states that \mathcal{R}_3 is of a certain Vapnik-Chervonenkis class [see Definition 2.1 of Chernozhukov et al., 2014]. Assumption 12 imposes high-level conditions on the convergence rates of the estimated nuisance functions when the cross-fitting technique is applied. Under proper conditions [see, Dikkala et al., 2020, for details], those obtained via (11) and (13) respectively can satisfy Assumption 12.

We further define the approximation error of r^* in terms of the ϕ -risk by

$$\mathbb{A}(\rho_{4,n}) = \inf_{r \in \mathcal{R}_3} \{R_\phi(r) + \rho_{4,n} \|r\|_{\mathcal{R}_3}^2\} - R_\phi(r^*),$$

and define the irreducible value gap between d_3^* and the global optimal ITR d^* by

$$\mathbb{G}(d_3^*) = V(d^*) - V(\text{sign}(d_3^*)).$$

For two positive sequences $\{a_n : n \geq 1\}$ and $\{b_n : n \geq 1\}$, we denote $a_n \lesssim b_n$ if $\limsup_{n \rightarrow \infty} a_n/b_n < \infty$.

The finite sample excess risk bound for \hat{d}_3^{DR} is given as follows.

Theorem 5.1. *Suppose that Assumptions 1-9 and 10-12 hold. If $\rho_{4,n} \leq 1$, then for any $x > 0$, with probability at least $1 - \exp(-x)$, we have*

$$\begin{aligned} V(d^*) - V(\hat{d}_3^{DR}) &\lesssim \mathbb{G}(d_3^*) + \mathbb{A}(\rho_{4,n}) + \sqrt{v}\rho_{4,n}^{-1/2}n^{-1/2} \\ &\quad + \max\{1, x\}n^{-(\alpha+\beta)}\rho_{4,n}^{-1/2} + \max\{1, x\}\sqrt{vn}^{-1/2-\min\{\alpha,\beta\}}\rho_{4,n}^{-1/2}. \end{aligned} \quad (24)$$

The proof of Theorem 5.1 is given in Supplementary Material S2. Theorem 5.1 shows that the finite sample excess risk bound for \hat{d}_3^{DR} consists of four components. The first component $\mathbb{G}(d_3^*)$ is an irreducible error due to unmeasured confounding. The second component is the approximation error $\mathbb{A}(\rho_{4,n})$ determined by the size of \mathcal{R}_3 and tuning parameter $\rho_{4,n}$. The third component $\sqrt{v}\rho_{4,n}^{-1/2}n^{-1/2}$ is the estimation error with respect to \mathcal{R}_3 assuming the nuisance functions are known. The last two components, $\max\{1, x\}n^{-(\alpha+\beta)}\rho_{4,n}^{-1/2}$ and $\max\{1, x\}\sqrt{vn}^{-1/2-\min\{\alpha,\beta\}}\rho_{4,n}^{-1/2}$ are the errors due to estimating the nuisance functions h_0 and q_0 . These two errors are negligible if $\alpha + \beta > \frac{1}{2}$, which can be guaranteed by many nonparametric estimators, including those defined in (11) and (13).

The finite sample error bounds for other proposed proximal learning methods can be similarly derived and are thus omitted here for brevity. Similar to that for \hat{d}_3^{DR} , each of their value difference bounds can be decomposed into aforementioned four components. The magnitude of the irreducible error due to unmeasured confounding is determined by the size of the corresponding identifiable class of treatment regimes. Obviously the irreducible error related to d_4^* is the smallest but at the expense of making additional untestable assumptions. The approximation and estimation errors with respect to different pre-specified classes of treatment regimes are similar for all our proposed methods. The errors incurred by estimating nuisance functions vary among these methods and they depend on the assumptions imposed on the nuisance function estimation. While the result in Theorem 5.1 is similar to those from Zhao et al. [2019], we consider the ITR estimation problem under the existence of unmeasured confounders while Zhao et al. [2019] considered the no unmeasured confounding scenario. Therefore, the assumptions and proofs for obtaining our result are substantially different from those in Zhao et al. [2019].

6 Simulation

In this section we perform a simulation study to evaluate the numerical performance of our proposed optimal ITR estimators with unmeasured confounding, where a representative existing estimator under no unmeasured confounding [Zhao et al., 2019] and an *oracle* estimator that can access the unmeasured confounders are compared. Due to the length of presentation, we only report key simulation results in this section. Implementation details and additional numerical results such as statistical inference related to $V(d_3)$ for $d_3 \in \mathcal{D}_3$ can be found in the Supplementary Material.

6.1 Simulated Data Generation

Here we briefly describe our simulated data generating mechanism, which is motivated by Cui et al. [2020]. The details are given in Supplementary Material S4.

Step 1. We generate data (L, A, Z, W, U) by the following steps:

- 1.1 The covariates L are generated by $L \sim N([0.25, 0.25]^\top, \text{diag}\{0.25^2, 0.25^2\})$. The treatment A is generated by a Bernoulli distribution with

$$\Pr(A = 1 | L) = [1 + \exp\{[0.125, 0.125]L\}]^{-1}.$$

As shown in Supplementary Material S4, this is compatible with

$$\Pr(A = 1 | U, L) = [1 + \exp\{0.09375 + [0.1875, 0.1875]L - 0.25U\}]^{-1}, \quad (25)$$

where U is generated below.

- 1.2 Then we generate (Z, W, U) by the following conditional multivariate normal distribution given (A, L) with parameters given in Supplementary Material S4:

$$(Z, W, U) | (A, L) \sim N \left(\begin{bmatrix} \alpha_0 + \alpha_a \mathbb{I}(A = 1) + \alpha_l^\top L \\ \mu_0 + \mu_a \mathbb{I}(A = 1) + \mu_l^\top L \\ \kappa_0 + \kappa_a \mathbb{I}(A = 1) + \kappa_l^\top L \end{bmatrix}, \begin{bmatrix} \sigma_z^2 & \sigma_{zw} & \sigma_{zu} \\ \sigma_{zw} & \sigma_w^2 & \sigma_{wu} \\ \sigma_{zu} & \sigma_{wu} & \sigma_u^2 \end{bmatrix} \right).$$

As shown in Supplementary Material S4, they lead to the following compatible model of q_0 :

$$q_0(Z, A, L) = 1 + \exp \left\{ A(t_0 + t_z Z + t_a \mathbb{I}(A = 1) + t_l^\top L) \right\},$$

where the values of t_0, t_z, t_a and t_l are specified in Supplementary Material S4.

Step 2. Based on the generated (L, A, Z, W, U) , we generate Y by adding a random noise from the uniform distribution on $[-1, 1]$ to

$$\begin{aligned} \mathbb{E}(Y \mid W, U, A, Z, L) &= \mathbb{E}(Y \mid U, A, Z, L) + \omega \{W - \mathbb{E}(W \mid U, A, Z, L)\} \\ &= \mathbb{E}(Y \mid U, A, L) + \omega \{W - \mathbb{E}(W \mid U, L)\}, \end{aligned}$$

of which details will be specified in different scenarios below.

Next we consider the following outcome confounding bridge function h_0 , which leads to a linear decision function of d_1^* . We let

$$\begin{aligned} h_0(W, A, L) &= c_0 + c_1 \mathbb{I}(A = 1) + c_2 W + c_3^\top L + \mathbb{I}(A = 1)(c_4 W + c_5^\top L), \text{ and thus} \\ \mathbb{E}(Y \mid W, U, A, Z, L) &= c_0 + c_1 \mathbb{I}(A = 1) + c_3^\top L + \mathbb{I}(A = 1)c_5^\top L + \omega W \\ &\quad + \{c_2 + c_4 \mathbb{I}(A = 1) - \omega\} \left\{ \mu_0 + \mu_l^\top L + \frac{\sigma_{wu}}{\sigma_u^2} (U - \kappa_0 - \kappa_l^\top L) \right\}, \end{aligned}$$

where the values of c_0 – c_5 and ω are specified in Table 3 and the other parameters are given in Supplementary Material S4. Accordingly the global optimal ITR is

$$\begin{aligned} d^*(L, U) &= \text{sign}[\mathbb{E}(Y \mid L, U, A = 1) - \mathbb{E}(Y \mid L, U, A = -1)] \\ &= \text{sign} \left[c_1 + c_5^\top L + c_4 \left\{ \mu_0 + \mu_l^\top L + \frac{\sigma_{wu}}{\sigma_u^2} (U - \kappa_0 - \kappa_l^\top L) \right\} \right]. \end{aligned}$$

As shown in Table 3, we consider two scenarios. In Scenario L1, the global optimal ITR cannot be identified, but the outcome bridge difference $\Delta = h_0(W, 1, L) - h_0(W, -1, L)$ depends on both W and L , so taking W or Z into account can potentially improve the value function if identifiable. In Scenario L2, the global optimal ITR only depends on L , which thus can be identified under our

proximal learning framework.

Table 3: Simulation scenarios for linear h_0 .

Scenario	c_0	c_1	c_2	c_3	c_4	c_5	ω
L1	2	0.5	8	$[0.25, 0.25]^\top$	0.25	$[3, -5]^\top$	2
L2	2	0.5	8	$[0.25, 0.25]^\top$	0	$[3, -5]^\top$	2

We also consider a second case where h_0 is a nonlinear function of L and W . We let

$$h_0(W, A, L) = c_0 + c_1(A) + c_2W + c_3(L) + \mathbb{I}(A = 1) \{c_4W + c_5(L) + Wc_6(L)\}, \text{ and thus}$$

$$\mathbb{E}(Y | W, U, A, Z, L) = c_0 + c_1(A) + c_3(L) + \mathbb{I}(A = 1)c_5(L) + \omega W$$

$$+ \{c_2 + c_4\mathbb{I}(A = 1) + Ac_6(L) - \omega\} \left\{ \mu_0 + \mu_l^\top L + \frac{\sigma_{wu}}{\sigma_u^2}(U - \kappa_0 - \kappa_l^\top L) \right\},$$

where functions c_1, c_3, c_5, c_6 , and values of c_0, c_2, c_4 and ω are specified in Table 4 and the other parameters are given in Supplementary Material. Accordingly the global optimal ITR is

$$d^*(L, U) = \text{sign}[\mathbb{E}(Y | L, U, A = 1) - \mathbb{E}(Y | L, U, A = -1)]$$

$$= \text{sign} \left[c_1(1) - c_1(-1) + c_5(L) + [c_4 + c_6(L)] \left\{ \mu_0 + \mu_l^\top L + \frac{\sigma_{wu}}{\sigma_u^2}(U - \kappa_0 - \kappa_l^\top L) \right\} \right].$$

Table 4: Simulation scenarios for nonlinear h_0 .

Scenario	c_0	$c_1(A)$	c_2	$c_3(L)$	c_4	$c_5(L)$	$c_6(L)$	ω
N1	2	$2.3\mathbb{I}(A = 1)$	4	$L^\top L$	-2.5	$ L_1 - 1 - L_2 + 1 $	$\sin L_1 - 2 \cos L_2$	2
N2	2	$0.25\mathbb{I}(A = 1)$	5	$L^\top L$	0	$-6L_1L_2$	0	2

These two scenarios N1 and N2 shown in Table 4 are analogous to L1 and L2 in Table 3. In each simulation setting described above, we have 100 simulation runs with $n = 2,000$ and $5,000$ subjects in each run, and also generate a *noise-free* test dataset of 500,000 used to obtain values of estimated ITRs by (2) with (25).

6.2 Estimators and Implementations

To increase the difficulty of this simulation study, we added eight independent variables from the

uniform distribution on $[-1, 1]$ in L and used the resulting concatenated 10-dimensional L in all ITR learning methods.

We implement all four proposed learning methods in Table 2 denoted by $d1(L, Z)$, $d2(L, W)$, $d3DR(L)$ and $d4$ here respectively, together with an optimal ITR estimator denoted by $d1(L)$ here, which is assumed to only depend on L and obtained by (15), as well as the optimal ITR estimator $d2(L)$, which is assumed to only depend on L and obtained by (16). The latter two are used to compared with $d3DR(L)$. We also compare our proposed optimal ITR estimators with that by efficient augmentation and relaxation learning [EARL, Zhao et al., 2019] designed under no unmeasured confounding. We denote it by $dEARL(L)$ here and implement it using the R package `DynTxRegime`. To obtain $dEARL(L)$ when U is unobserved, we use all observed variables (L, W, Z) to construct tree-based nonparametric main effect models and propensity score models, and then fit the regime in terms of L . We also create an oracle optimal ITR estimator, denoted by NUC , which is obtained by EARL using (L, U) . Due to the relatively unsatisfactory computing speed of the R package `DynTxRegime`, we only obtain $dEARL(L)$ and NUC in Scenarios L1 and L2 but not in Scenarios N1 and N2. For L2 scenario, we only use L to construct an ITR for NUC since the optimal one only depends on L . Note that NUC is unattainable in practice since U is unobserved, but it can be regarded as a benchmark estimator for comparison.

We use the quadratic smoothed hinge loss as surrogate $\phi(\cdot)$ for all proximal learners. The nuisance functions involved in our proposed methods, i.e., the confounding bridge functions h_0 and q_0 , are estimated by (11) and (13), respectively, with RKHSs $\mathcal{F}, \mathcal{H}, \mathcal{G}$, and \mathcal{Q} all equipped with Gaussian kernels. For Scenarios L1 and L2, all decision functions are fitted as linear functions of their corresponding covariates with the ℓ_2 penalty on coefficients. For Scenarios N1 and N2, $\mathcal{R}_1, \mathcal{R}_2$, and \mathcal{R}_3 are chosen as RKHSs equipped with Gaussian kernels. Tuning parameters of the penalties are selected by cross-validation (see Supplementary Material S3 for details). For computational acceleration, all kernels are approximated by the Nyström method with $2\lceil\sqrt{n}\rceil$ features [Yang et al., 2012].

6.3 Simulation Results

The values of all optimal ITR estimates for $n = 5,000$ are illustrated in Figures 4-5. The figures for $n = 2,000$ and detailed comparisons with EARL are given in Supplementary Material S5.

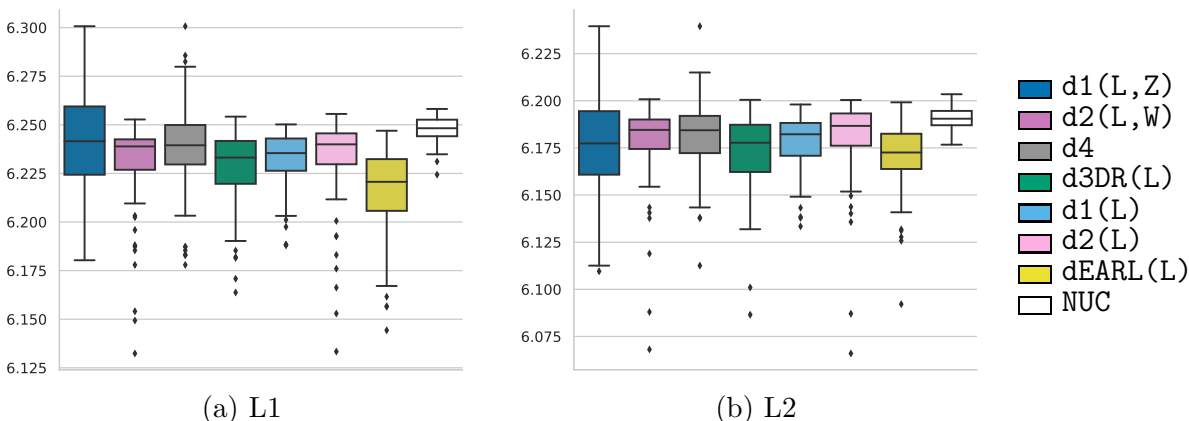


Figure 4: Boxplots of values for Scenario L1 and L2 with sample size $n = 5,000$.

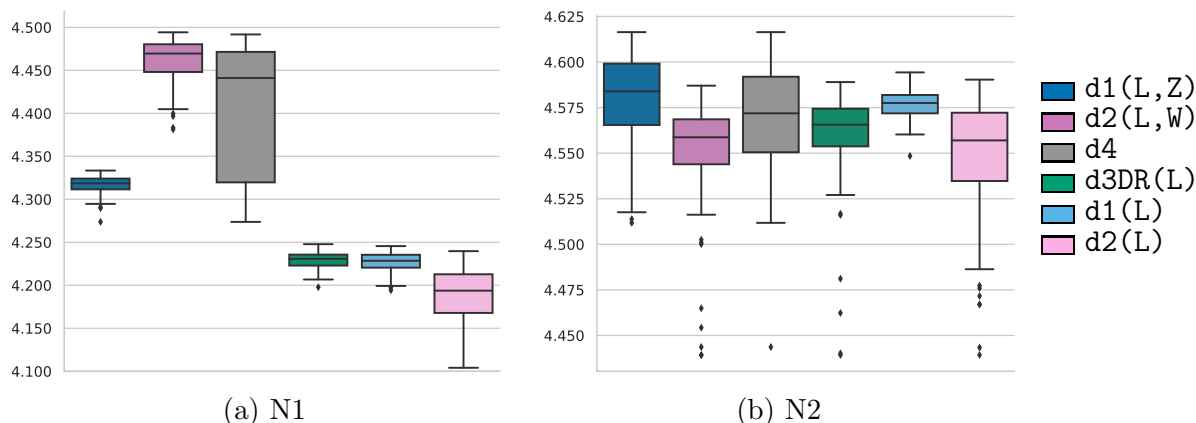


Figure 5: Boxplots of values for Scenario N1 and N2 with sample size $n = 5,000$

Figure 4 shows that the oracle estimator NUC is the best in Scenarios L1 and L2. This is not surprising since in Scenario L1 the global optimal ITR cannot be identified by the other methods based on observed data. In comparison, since U is unobserved but $\text{dEARL}(L)$ is developed under no unmeasured confounding, as expected, all our proposed methods have better values than $\text{dEARL}(L)$. In Scenarios L1 and N1, $\text{d1}(L,Z)$ and $\text{d2}(L,W)$ outperform $\text{d1}(L)$ and $\text{d2}(L)$ respectively, which demonstrates the improvement of decision making by including the proxy variables Z and W when the optimal decisions depend on unobserved U .

For Scenarios L2 and N2, the global optimal ITR can be identified by our proposed methods

since the difference of outcome bridge only depends on L . Figure 4 (b) shows that all our proposed methods are comparable to NUC in Scenario L2 but the values of $dEARL(L)$ are less satisfactory. Figure 4 also shows that $d1(L)$, $d2(L)$ and $d3DR(L)$ have similar performances in Scenario L2 while $d1(L,Z)$, $d2(L,W)$ and $d4$ lead to values with slightly or substantially higher variations. This is consistent with the fact that the global optimal ITR only depends on L in Scenario L2 so adding Z or W into an ITR may only increase its variability. For Scenario N2, similar patterns can be discovered in Figure 5 (b). The values of the maximum proximal estimator $d4$ mostly lie between those of $d1(L,Z)$ and of $d2(L,W)$. These observations are intuitively reasonable and consistent with the discussion in Section 4 above.

In all scenarios, the optimal ITR estimators which involve estimating q_0 typically have relatively longer lower shadows. Therefore, it is an interesting future research direction to study how to improve the practical performance of treatment proximal learning method.

7 Real Data Application

In this section, we apply the five proposed proximal learning methods to a dataset from the Study to Understand Prognoses and Preferences for Outcomes and Risks of Treatments [SUPPORT, Connors et al., 1996]. SUPPORT examined the effectiveness and safety of direct measurement of cardiac function by Right Heart Catheterization (RHC) for certain critically ill patients in intensive care units (ICU). This dataset has been analyzed mainly to estimate the average treatment effect of using RHC [e.g., Lin et al., 1998, Tan, 2006, Tchetgen Tchetgen et al., 2020, Cui et al., 2020].

Our objective is to find an optimal ITR on the usage of RHC that maximizes 30-day survival rates of critically ill patients from the day admitted or transferred to ICU. The data include 5,735 patients, of whom 2,184 were measured by RHC in the first 24 hours ($A = 1$) and 3,551 were in the control group ($A = -1$). Finally, 3,817 patients survived or censored at day 30 ($Y = 1$) and 1,918 died within 30 days ($Y = -1$). For each individual, we consider 71 covariates including demographics, diagnosis, estimated survival probability, comorbidity, vital signs, and physiological status among others. See the full list of covariates in <https://hbiostat.org/data/repo/rhc.html>. During the first 24 hours in the ICU, ten variables were measured from a blood test for the assessment of the physiological status. Following

Tchetgen Tchetgen et al. [2020], among those ten physiological status, we let $Z = (\text{pafi1}, \text{paco21})$ be treatment-inducing confounding proxies and $W = (\text{ph1}, \text{hema1})$ be outcome-inducing confounding proxies respectively, where `pafi1` is the ratio of arterial oxygen partial pressure to fractional inspired oxygen, `paco21` is the partial pressure of carbon dioxide, `ph1` is arterial blood pH, `hema1` is hematocrit. We apply our proposed methods to obtain $d1(L, Z)$, $d2(L, W)$, $d3DR(L)$, $d1(L)$ and $d2(L)$ using this dataset with the same configurations of Scenarios L1 and L2 in Section 6.

The coefficient estimates of all covariates are given in Supplementary Material S6. In Table 5, we provide a selected number of them with the relatively large coefficient estimates in absolute value. First, the negative intercepts in Table 5 indicates that RHC may have a potential negative averaged treatment effect on the 30-day survival rate for critically ill patients, which is consistent with the existing literature [e.g., Tan, 2006]. Second, the negative coefficients of `surv2md1` suggest not perform RHC to a patient with a higher survival prediction on day 1. In contrast, our estimated ITRs tend to suggest trauma patients (`trauma`), and patients diagnosed with coma (`cat1_coma`, `cat2_coma`), lung cancer (`cat1_lung`, `cat2_lung`) or congestive heart failure (`cat1_chf`) undergo RHC. Clinically, RHC is of value when the hemodynamic state of a patient is in question or changing rapidly and is thus potentially helpful with patients in critical condition whose hemodynamic states are unstable [Kubiak et al., 2019]. Those findings can be partially supported by Hernandez et al. [2019] and Tehrani et al. [2019], but require further investigations. Our estimated ITRs also imply that patients with upper gastrointestinal bleeding (`gibledhx`) or autoimmune polyglandular syndrome type 3 (`aps1`) might be harmed by RHC, which is also worthy of future studies.

The treatment recommendations by the five estimated ITRs for all 5,735 patients, as illustrated in Figure 6, show some discrepancies among them. The estimated ITR by doubly robust proximal learning, $d3DR(L)$, only suggests 675 patients to receive RHC, the smallest number among the five. The estimated ITRs by outcome proximal learning, $d1(L, Z)$ and $d1(L)$, both suggest a similar group of around 1,400 patients receive RHC, while those by treatment proximal learning, $d2(L, W)$ and $d2(L)$, suggest RHC to a similar group of around 2,200 patients.

Due to the potentially different recommendations by the five estimated ITRs, one may conservatively suggest a patient to undergo RHC if, for example, at least four of them agree to recommend it, and accordingly obtain an ensemble ITR. Based on such ensemble ITR for the 5,735 patients as

Table 5: Important coefficients of estimated optimal ITRs. `surv2md1`: 2M model survival prediction at day 1; `gibledhx`: upper gastrointestinal bleeding; `aps1`: APS III ignoring coma at day 1; `cat1` and `cat2`: first and secondary disease category; `lung`: lung cancer; `chf`: congestive heart failure.

Covariate	d2(L,W)	d2(L)	d3DR(L)	d1(L)	d1(L,Z)
<code>intercept</code>	-0.204	-0.258	-0.722	-1.215	-1.222
<code>surv2md1</code>	-0.683	-0.699	-0.254	-0.747	-0.724
<code>gibledhx</code> (Yes=1/No=0)	-0.511	-0.490	-0.065	-0.343	-0.328
<code>aps1</code> (Yes=1/No=0)	-0.361	-0.405	-0.184	-0.451	-0.461
<code>trauma</code> (Yes=1/No=0)	0.862	0.925	0.020	0.622	0.533
<code>cat1_coma</code> (Yes=1/No=0)	-0.091	-0.112	0.215	2.183	2.210
<code>cat2_coma</code> (Yes=1/No=0)	0.261	0.248	0.092	2.059	2.009
<code>cat1_lung</code> (Yes=1/No=0)	-0.025	-0.098	0.062	1.740	1.711
<code>cat2_lung</code> (Yes=1/No=0)	0.960	1.131	0.033	1.412	1.072
<code>cat1_chf</code> (Yes=1/No=0)	0.757	0.731	-0.005	0.544	0.525

illustrated in Figure 6, we construct a decision tree as illustrated in Figure 7 to explore which covariates indicate the use of RHC. For example, patients in coma and those diagnosed with multiple organ system failure with malignancy are generally recommended to receive RHC in first 24 hours.

8 Discussions

In this paper, we propose several proximal learning methods to find optimal ITRs when there exists unmeasured confounding. Our methods are built upon the recently developed proximal causal inference. When the observed covariates can be decomposed into variables that are common causes of the outcome and treatment, namely outcome-inducing confounding proxies and treatment-inducing confounding proxies, we establish several identification results on a variety of classes of treatment regimes under different assumptions. Based on these results, we propose several classification-based approaches to estimating restricted in-class optimal ITRs. The superior performance of our methods is demonstrated by simulation, especially when the identification assumptions are satisfied. The real data application above shows the potential of the proposed methods to shed light on the recommended use of RHC on subgroups of patients, although this requires additional studies to demonstrate.

There are several interesting directions for future research. First, as shown in the simulation study, although a flexible nonparametric method is used to estimate q_0 to alleviate its model misspecification, the finite sample performance of most optimal ITR estimators involving estimated q_0 is not as good as

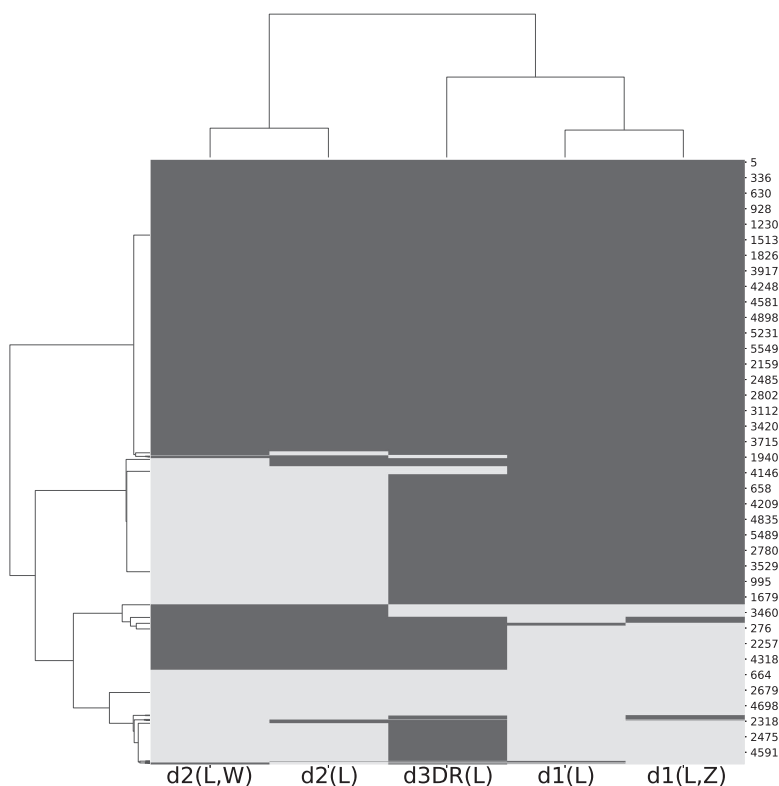


Figure 6: Optimal treatments suggested by the five estimated ITRs. Light portions represent that ITRs suggest the patients to undergo RHC while dark portions represent otherwise.

that of those involving estimated h_0 . This demonstrates the difficulty in estimating q_0 , analogous to that in estimating the propensity score in average treatment effect estimation under no unmeasured confounding. One possible approach to addressing this limitation is to develop weighted estimators similar to [Wong and Chan \[2017\]](#) and [Athey et al. \[2018\]](#). Moreover, our proposed methods are developed for a single decision time point. It will be interesting to extend them to the longitudinal data to estimate the optimal dynamic treatment regimes where individualized decisions are needed at multiple time points. This may be practically useful, e.g., to study the treatment of some chronic disease. It is also meaningful to study the estimation of optimal ITRs for survival outcomes in the presence of unmeasured confounding.

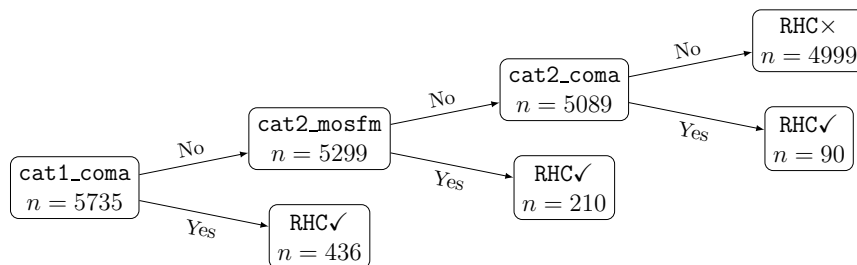


Figure 7: Decision tree of RHC based on the ensemble ITR, which recommends a patient to undergo RHC if at least four of the estimated ITRs all recommend it. `mosfm`: multiple organ system failure with malignancy.

Supplementary Material

All technical proofs, implementation details and additional numerical results are given in Supplementary Material.

References

- C. Ai and X. Chen. Efficient estimation of models with conditional moment restrictions containing unknown functions. *Econometrica*, 71(6):1795–1843, 2003.
- S. Athey and S. Wager. Policy learning with observational data. *Econometrica*, 89(1):133–161, 2021.
- S. Athey, G. W. Imbens, and S. Wager. Approximate residual balancing: debiased inference of average treatment effects in high dimensions. *Journal of the Royal Statistical Society: Series B (Statistical Methodology)*, 80(4):597–623, 2018.
- P. J. Bickel. On adaptive estimation. *Annals of Statistics*, pages 647–671, 1982.
- R. Blundell, X. Chen, and D. Kristensen. Semi-nonparametric IV estimation of shape-invariant Engel curves. *Econometrica*, 75(6):1613–1669, 2007.
- G. Chamberlain. Efficiency bounds for semiparametric regression. *Econometrica*, 60(3):567–596, 1992.
- G. Chen, D. Zeng, and M. R. Kosorok. Personalized dose finding using outcome weighted learning. *Journal of the American Statistical Association*, 111(516):1509–1521, 2016.
- X. Chen. Large sample sieve estimation of semi-nonparametric models. *Handbook of econometrics*, 6: 5549–5632, 2007.
- X. Chen and D. Pouzo. Estimation of nonparametric conditional moment models with possibly non-smooth generalized residuals. *Econometrica*, 80(1):277–321, 2012.
- X. Chen, V. Chernozhukov, S. Lee, and W. K. Newey. Local identification of nonparametric and semiparametric models. *Econometrica*, 82(2):785–809, 2014.
- V. Chernozhukov, D. Chetverikov, K. Kato, et al. Gaussian approximation of suprema of empirical processes. *Annals of Statistics*, 42(4):1564–1597, 2014.

- V. Chernozhukov, D. Chetverikov, M. Demirer, E. Duflo, C. Hansen, W. Newey, and J. Robins. Double/debiased machine learning for treatment and structural parameters. *The Econometrics Journal*, 21:1–68, 2018.
- J. Connors, Alfred F., T. Speroff, N. V. Dawson, C. Thomas, J. Harrell, Frank E., D. Wagner, N. Desbiens, L. Goldman, A. W. Wu, R. M. Califf, J. Fulkerson, William J., H. Vidaillet, S. Broste, P. Bellamy, J. Lynn, and W. A. Knaus. The Effectiveness of Right Heart Catheterization in the Initial Care of Critically III Patients. *Journal of the American Medical Association*, 276(11):889–897, 09 1996. ISSN 0098-7484.
- Y. Cui and E. J. Tchetgen Tchetgen. A semiparametric instrumental variable approach to optimal treatment regimes under endogeneity. *Journal of the American Statistical Association*, pages 1–12, 2020.
- Y. Cui, H. Pu, X. Shi, W. Miao, and E. J. Tchetgen Tchetgen. Semiparametric proximal causal inference. *arXiv preprint arXiv:2011.08411*, 2020.
- B. B. Damodaran. Fast Optimal Bandwidth Selection for RBF Kernel using Reproducing Kernel Hilbert Space Operators for Kernel Based Classifiers. *arXiv preprint arXiv:1804.05214*, 2018.
- X. D’Haultfoeuille. On the completeness condition in nonparametric instrumental problems. *Econometric Theory*, pages 460–471, 2011.
- N. Dikkala, G. Lewis, L. Mackey, and V. Syrgkanis. Minimax estimation of conditional moment models. *arXiv preprint arXiv:2006.07201*, 2020.
- M. Dudík, J. Langford, and L. Li. Doubly robust policy evaluation and learning. *arXiv preprint arXiv:1103.4601*, 2011.
- K. Fukumizu, A. Gretton, G. Lanckriet, B. Schölkopf, and B. K. Sriperumbudur. Kernel Choice and Classifiability for RKHS Embeddings of Probability Distributions. In Y. Bengio, D. Schuurmans, J. Lafferty, C. Williams, and A. Culotta, editors, *Advances in Neural Information Processing Systems*, volume 22. Curran Associates, Inc., 2009.
- A. Ghassami, A. Ying, I. Shpitser, and E. J. Tchetgen Tchetgen. Minimax Kernel Machine Learning for a Class of Doubly Robust Functionals. *arXiv preprint arXiv:2104.02929*, 2021.
- S. Han. Optimal Dynamic Treatment Regimes and Partial Welfare Ordering. *arXiv preprint arXiv:1912.10014*, 2019.
- G. A. Hernandez, A. Lemor, V. Blumer, C. A. Rueda, S. Zalawadiya, L. W. Stevenson, and J. Lindenfeld. Trends in utilization and outcomes of pulmonary artery catheterization in heart failure with and without cardiogenic shock. *Journal of cardiac failure*, 25(5):364–371, 2019.
- N. Kallus, X. Mao, and M. Uehara. Causal Inference Under Unmeasured Confounding With Negative Controls: A Minimax Learning Approach. *arXiv preprint arXiv:2103.14029*, 2021.
- P. Klasnja, E. B. Hekler, S. Shiffman, A. Boruvka, D. Almirall, A. Tewari, and S. A. Murphy. Microrandomized trials: An experimental design for developing just-in-time adaptive interventions. *Health Psychology*, 34(S):1220, 2015.
- J. Kober, J. A. Bagnell, and J. Peters. Reinforcement learning in robotics: A survey. *The International Journal of Robotics Research*, 32(11):1238–1274, 2013.

- M. R. Kosorok and E. B. Laber. Precision medicine. *Annual Review of Statistics and Its Application*, 6:263–286, 2019.
- R. Kress, V. Maz'ya, and V. Kozlov. *Linear integral equations*, volume 82. Springer, 1989.
- G. M. Kubiak, A. Ciarka, M. Biniecka, and P. Ceranowicz. Right heart catheterization—background, physiological basics, and clinical implications. *Journal of clinical medicine*, 8(9):1331, 2019.
- D. Y. Lin, B. M. Psaty, and R. A. Kronmal. Assessing the sensitivity of regression results to unmeasured confounders in observational studies. *Biometrics*, pages 948–963, 1998.
- C. F. Manski. Statistical treatment rules for heterogeneous populations. *Econometrica*, 72(4):1221–1246, 2004.
- W. Miao and E. J. Tchetgen Tchetgen. A Confounding Bridge Approach for Double Negative Control Inference on Causal Effects. *arXiv preprint arXiv:1808.04945*, 2018.
- W. Miao, Z. Geng, and E. J. Tchetgen Tchetgen. Identifying causal effects with proxy variables of an unmeasured confounder. *Biometrika*, 105(4):987–993, 2018.
- W. K. Newey and J. L. Powell. Instrumental variable estimation of nonparametric models. *Econometrica*, 71(5):1565–1578, 2003.
- J. Pearl. *Causality*. Cambridge university press, 2009.
- H. Pu and B. Zhang. Estimating Optimal Treatment Rules with an Instrumental Variable: A Semi-Supervised Learning Approach. *arXiv preprint arXiv:2002.02579*, 2020.
- M. Qian and S. A. Murphy. Performance guarantees for individualized treatment rules. *Annals of Statistics*, 39(2):1180, 2011.
- H. Qiu, M. Carone, E. Sadikova, M. Petukhova, R. C. Kessler, and A. Luedtke. Optimal individualized decision rules using instrumental variable methods. *Journal of the American Statistical Association*, pages 1–18, 2020.
- N. U. Rashid, D. J. Lockett, J. Chen, M. T. Lawson, L. Wang, Y. Zhang, E. B. Laber, Y. Liu, J. J. Yeh, D. Zeng, and M. R. Kosorok. High-Dimensional Precision Medicine From Patient-Derived Xenografts. *Journal of the American Statistical Association*, 0(0):1–15, 2020.
- J. Robins. A new approach to causal inference in mortality studies with a sustained exposure period—application to control of the healthy worker survivor effect. *Mathematical Modelling*, 7(9-12):1393–1512, 1986.
- K. Seong, M. Mohseni, and J. M. Cioffi. Optimal resource allocation for OFDMA downlink systems. In *2006 IEEE International Symposium on Information Theory*, pages 1394–1398. IEEE, 2006.
- C. Shi, A. Fan, R. Song, and W. Lu. High-dimensional A-learning for optimal dynamic treatment regimes. *Annals of Statistics*, 46(3):925, 2018.
- X. Shi, W. Miao, J. C. Nelson, and E. J. Tchetgen Tchetgen. Multiply robust causal inference with double-negative control adjustment for categorical unmeasured confounding. *Journal of the Royal Statistical Society: Series B (Statistical Methodology)*, 82(2):521–540, 2020.

- L. Song, A. Smola, A. Gretton, J. Bedo, and K. Borgwardt. Feature selection via dependence maximization. *Journal of Machine Learning Research*, 13(5), 2012.
- Z. Tan. A distributional approach for causal inference using propensity scores. *Journal of the American Statistical Association*, 101(476):1619–1637, 2006.
- E. J. Tchetgen Tchetgen, A. Ying, Y. Cui, X. Shi, and W. Miao. An Introduction to Proximal Causal Learning. *arXiv preprint arXiv:2009.10982*, 2020.
- B. N. Tehrani, A. G. Truesdell, M. W. Sherwood, S. Desai, H. A. Tran, K. C. Epps, R. Singh, M. Psotka, P. Shah, L. B. Cooper, et al. Standardized team-based care for cardiogenic shock. *Journal of the American college of cardiology*, 73(13):1659–1669, 2019.
- L. Wang, Y. Zhou, R. Song, and B. Sherwood. Quantile-optimal treatment regimes. *Journal of the American Statistical Association*, 113(523):1243–1254, 2018.
- C. J. Watkins and P. Dayan. Q-learning. *Machine Learning*, 8(3-4):279–292, 1992.
- R. K. Wong and K. C. G. Chan. Kernel-based covariate functional balancing for observational studies. *Biometrika*, 105(1):199–213, 2017.
- T. Yang, Y.-F. Li, M. Mahdavi, R. Jin, and Z.-H. Zhou. Nyström method vs random fourier features: A theoretical and empirical comparison. *Advances in Neural Information Processing Systems*, 25: 476–484, 2012.
- B. Zhang, A. A. Tsiatis, E. B. Laber, and M. Davidian. A robust method for estimating optimal treatment regimes. *Biometrics*, 68(4):1010–1018, 2012.
- Y. Zhao, M. R. Kosorok, and D. Zeng. Reinforcement learning design for cancer clinical trials. *Statistics in medicine*, 28(26):3294–3315, 2009.
- Y. Zhao, D. Zeng, A. J. Rush, and M. R. Kosorok. Estimating individualized treatment rules using outcome weighted learning. *Journal of the American Statistical Association*, 107(499):1106–1118, 2012.
- Y.-Q. Zhao, D. Zeng, E. B. Laber, R. Song, M. Yuan, and M. R. Kosorok. Doubly robust learning for estimating individualized treatment with censored data. *Biometrika*, 102(1):151–168, 2014.
- Y.-Q. Zhao, E. B. Laber, Y. Ning, S. Saha, and B. E. Sands. Efficient augmentation and relaxation learning for individualized treatment rules using observational data. *Journal of Machine Learning Research*, 20(48):1–23, 2019.
- X. Zhou, N. Mayer-Hamblett, U. Khan, and M. R. Kosorok. Residual weighted learning for estimating individualized treatment rules. *Journal of the American Statistical Association*, 112(517):169–187, 2017.

A Example Illustration

In this section, we provide a concrete example to show how one can obtain restricted in-class optimal ITR via h_0 in Section 3.2.

Example 1. Let W, L, U and Z be all one-dimensional variables, and suppose that

$$\mathbb{E}(Y | A, Z, L, U) = b_0 + b_1A + b_2U + b_3L + A(b_4U + b_5L),$$

$$\mathbb{E}(W | A, Z, L, U) = a_0 + a_1U + a_2L,$$

where b_0 - b_5 , and a_0 - a_2 are some constants. Then we can show that

$$\mathbb{E}(Y | A, Z, L) = b_0 + b_1A + b_2\mathbb{E}(U | A, Z, L) + b_3L + A\{b_4\mathbb{E}(U | A, Z, L) + b_5L\},$$

$$\mathbb{E}(W | A, Z, L) = a_0 + a_1\mathbb{E}(U | A, Z, L) + a_2L.$$

If $a_1 \neq 0$, this implies that

$$\mathbb{E}(Y | A, Z, L) = c_0 + c_1A + c_2\mathbb{E}(W | A, Z, L) + c_3L + A\{c_4\mathbb{E}(W | A, Z, L) + c_5L\},$$

where $c_0 = b_0 - (a_0b_2)/a_1$, $c_1 = b_1 - (a_0b_4)/a_1$, $c_2 = b_2/a_1$, $c_3 = b_3 - (b_2a_2)/a_1$, $c_4 = b_4/a_1$ and $c_5 = b_5 - (a_2b_4)/a_1$. We can also observe that

$$h_0(W, A, L) = c_0 + c_1A + c_2W + c_3L + A(c_4W + c_5L),$$

and for any $d_1 \in \mathcal{D}_1$,

$$V(d_1) = c_0 + \mathbb{E}\{[c_1d_1(L, Z) + c_2W + c_3L + d_1(L, Z)(c_4W + c_5L)]\}.$$

Then d_1^* is

$$\begin{aligned} d_1^*(L, Z) &= \text{sign} [\mathbb{E} \{h_0(W, 1, L) \mid L, Z\} - \mathbb{E} \{h_0(W, -1, L) \mid L, Z\}] \\ &= \text{sign} \{c_1 + c_4 \mathbb{E}(W \mid L, Z) + c_5 L\}, \end{aligned} \tag{26}$$

almost surely.

B Technical Proofs

Proof of Theorem 3.1: Based on the definition of $V(d)$, we have the following equation for any $d_1 \in \mathcal{D}_1$:

$$V(d_1) = \mathbb{E} [Y(1)\mathbb{I}(d_1(L, Z) = 1) + Y(-1)\mathbb{I}(d_1(L, Z) = -1)]. \tag{27}$$

We can first show that

$$\begin{aligned} \mathbb{E} [Y(1)\mathbb{I}(d_1(L, Z) = 1)] &= \mathbb{E} [\mathbb{E} [Y(1) \mid L, Z] \mathbb{I}(d_1(L, Z) = 1)] \\ &= \mathbb{E} [\mathbb{E} [\mathbb{E} [Y(1) \mid L, U, Z] \mid L, Z] \mathbb{I}(d_1(L, Z) = 1)] \\ &= \mathbb{E} [\mathbb{E} [\mathbb{E} [Y \mid L, U, A = 1] \mid L, Z] \mathbb{I}(d_1(L, Z) = 1)] \\ &= \mathbb{E} [\mathbb{E} [\mathbb{E} [h_0(W, 1, L) \mid L, U] \mid L, Z] \mathbb{I}(d_1(L, Z) = 1)] \\ &= \mathbb{E} [\mathbb{E} [\mathbb{E} [h_0(W, 1, L) \mid L, U, Z] \mid L, Z] \mathbb{I}(d_1(L, Z) = 1)] \\ &= \mathbb{E} [h_0(W, 1, L)\mathbb{I}(d_1(L, Z) = 1)], \end{aligned}$$

where the third equality is due to Assumption 5, the fourth equality is shown by Theorem 1 of Miao et al. [2018] under Assumptions 6 (a) and 7, and the last but second equality is also due to Assumption 5.

Similarly, we can show that

$$\mathbb{E}[Y(-1)\mathbb{I}(d_1(L, Z) = -1)] = \mathbb{E}[h_0(W, -1, L)\mathbb{I}(d_1(L, Z) = -1)],$$

which concludes the first statement of Theorem 3.1. As we can see that

$$V(d_1) = E[h_0(W, -1, L)\mathbb{I}(d_1(L, Z) = -1)] + E[h_0(W, 1, L)\mathbb{I}(d_1(L, Z) = 1)],$$

then by minimizing $V(d_1)$ over \mathcal{D}_1 we can show that

$$d_1^*(L, Z) = \text{sign}(E[h_0(W, 1, L) | L, Z] - E[h_0(W, -1, L) | L, Z]),$$

almost surely.

Proof of Theorem 3.2: Based on the definition of $V(d)$, we have the following equation for any $d_2 \in \mathcal{D}_2$:

$$V(d_2) = \mathbb{E}[Y(1)\mathbb{I}(d_2(L, W) = 1) + Y(-1)\mathbb{I}(d_2(L, W) = -1)]. \quad (28)$$

Note that $A \perp\!\!\!\perp (Y(a), W) | (U, L)$ for $a \in \mathcal{A}$. We can first show that

$$\begin{aligned} & \mathbb{E}[Y(1)\mathbb{I}(d_2(L, W) = 1)] \\ &= \mathbb{E}[\mathbb{E}[Y(1) | L, W] \mathbb{I}(d_2(L, W) = 1)] \\ &= \mathbb{E}[\mathbb{E}[\mathbb{E}[Y(1) | L, U, W] | L, W] \mathbb{I}(d_2(L, W) = 1)] \\ &= \mathbb{E}[\mathbb{E}[\mathbb{E}[Y(1) | L, U, W, A = 1] | L, W] \mathbb{I}(d_2(L, W) = 1)], \end{aligned}$$

where the last equality is due to that $Y(a) \perp\!\!\!\perp A | (U, L, W)$. By the proof of Theorem 2.2 of [Cui et al. \[2020\]](#), we have

$$\mathbb{E}[q_0(Z, 1, L) | U, A = 1, L] \times \Pr(A = 1 | L, U) = 1.$$

This gives that

$$\begin{aligned}
& \mathbb{E} [Y(1)\mathbb{I}(d_2(L, W) = 1)] \\
&= \mathbb{E} [\mathbb{E} [\mathbb{E} [Y(1) | L, U, W, A = 1] \mathbb{E} [q_0(Z, 1, L) | U, A = 1, L] \times \Pr(A = 1 | L, U) | L, W] \mathbb{I}(d_2(L, W) = 1)] \\
&= \mathbb{E} [\mathbb{E} [\mathbb{E} [Y(1)q_0(Z, 1, L) | L, U, W, A = 1] \times \Pr(A = 1 | L, U) | L, W] \mathbb{I}(d_2(L, W) = 1)] \\
&= \mathbb{E} [\mathbb{E} [\mathbb{E} [Yq_0(Z, 1, L) | L, U, W, A = 1] \times \Pr(A = 1 | L, U, W) | L, W] \mathbb{I}(d_2(L, W) = 1)] \\
&= \mathbb{E} [\mathbb{E} [\mathbb{E} [Yq_0(Z, 1, L)\mathbb{I}(A = 1) | L, U, W] | L, W] \mathbb{I}(d_2(L, W) = 1)] \\
&= \mathbb{E} [Yq_0(Z, 1, L)\mathbb{I}(A = 1)\mathbb{I}(d_2(L, W) = 1)]
\end{aligned}$$

where the second equality is due to that $Z \perp\!\!\!\perp W | (U, L)$ and $Z \perp\!\!\!\perp Y(a) | (U, L, W, A)$ ensured by Assumption 5, and the third equality is based on that $A \perp\!\!\!\perp W | (U, L)$ by Assumption 5 and $Y = Y(A)$ almost surely in Assumption 1. Similarly, we can show that

$$\mathbb{E} [Y(-1)\mathbb{I}(d_2(L, W) = -1)] = \mathbb{E} [Y\mathbb{I}(A = -1)q_0(Z, -1, L)\mathbb{I}(d_2(L, W) = -1)],$$

and thus

$$\begin{aligned}
V(d_2) &= \mathbb{E} [Y\mathbb{I}(A = 1)q_0(Z, 1, L)\mathbb{I}(d_2(L, W) = 1) + Y\mathbb{I}(A = -1)q_0(Z, -1, L)\mathbb{I}(d_2(L, W) = -1)] \\
&= \mathbb{E} [Yq_0(Z, A, L)\mathbb{I}(d_2(L, W) = A)].
\end{aligned}$$

Following similar arguments in the proof of Theorem 3.1, we can further show that

$$d_2^*(L, W) = \text{sign} [\mathbb{E} \{Y\mathbb{I}(A = 1)q_0(Z, 1, L) | L, W\} - \mathbb{E} \{Y\mathbb{I}(A = -1)q_0(Z, -1, L) | L, W\}], \quad (29)$$

almost surely.

Proof of Proposition 5.1: Under some regularity condition, \hat{h}_0 and \hat{q}_0 converge in probability to \bar{h}_0 and \bar{q}_0 respectively in the sup-norm. Suppose $\bar{h}_0 = h_0$, i.e., h_0 is estimated consistently, then for

any $d \in \mathcal{D}_3$,

$$\begin{aligned}
& \mathbb{E} [C_1(Y, L, W, Z, A; h_0, \bar{q}_0)\mathbb{I}(d(L) = 1) + C_{-1}(Y, L, W, Z; h_0, \bar{q}_0)\mathbb{I}(d(L) = -1)] \\
&= \mathbb{E} [\mathbb{I}(A = d(L) = 1)\bar{q}_0(Z, 1, L)(Y - h_0(W, 1, L)) + \mathbb{I}(A = d(L) = -1)\bar{q}_0(Z, -1, L)(Y - h_0(W, -1, L))] \\
&+ V(d) \\
&= \mathbb{E} [P(A = 1|Z, L)\mathbb{I}(d(L) = 1)\bar{q}_0(Z, 1, L)\mathbb{E}[Y - h_0(W, 1, L) | Z, A = 1, L]] \\
&+ \mathbb{E} [P(A = -1|Z, L)\mathbb{I}(d(L) = -1)\bar{q}_0(Z, -1, L)\mathbb{E}[Y - h_0(W, -1, L) | Z, A = -1, L]] + V(d_3) \\
&= V(d),
\end{aligned}$$

where the last equality is due to (3) in Assumption 7. If $\bar{q}_0 = q_0$, i.e., q_0 can be estimated consistently, then

$$\begin{aligned}
& \mathbb{E} [C_1(Y, L, W, Z; h_0, \bar{q}_0)\mathbb{I}(d(L) = 1) + C_{-1}(Y, L, W, Z; h_0, \bar{q}_0)\mathbb{I}(d(L) = -1)] \tag{30} \\
&= \mathbb{E} [\mathbb{I}(A = d(L) = 1)q_0(Z, 1, L)Y] + \mathbb{E} [\mathbb{I}(A = d(L) = -1)q_0(Z, -1, L)Y] \\
&+ \mathbb{E} [\mathbb{I}(d(L) = 1)(1 - \mathbb{I}(A = 1)q_0(Z, 1, L))h_0(W, 1, L)] \\
&+ \mathbb{E} [\mathbb{I}(d(L) = -1)(1 - \mathbb{I}(A = -1)q_0(Z, -1, L))h_0(W, -1, L)] \\
&= \mathbb{E} [\mathbb{I}(d(L) = 1)Y(1) + \mathbb{I}(d(L) = -1)Y(-1)] \\
&+ \mathbb{E} [\mathbb{I}(d(L) = 1)(1 - \mathbb{E} [\mathbb{I}(A = 1)q_0(Z, 1, L) | W, L])h_0(W, 1, L)] \\
&+ \mathbb{E} [\mathbb{I}(d(L) = -1)(1 - \mathbb{E} [\mathbb{I}(A = -1)q_0(Z, -1, L) | W, L])h_0(W, -1, L)] \\
&= V(d),
\end{aligned}$$

where the first inequality is due to the proof of Theorem 3.2 and the last inequality is due to the fact that $\mathbb{E} [\mathbb{I}(A = a)q_0(Z, A, L) | W, L] = 1$.

Proof of Theorem 5.1: Without loss of generality, we assume that $C_1(Y, L, W, Z; h_0, q_0)$ and $C_{-1}(Y, L, W, Z; h_0, q_0)$ are both positive. For the ease of presentation, we use C_a and \hat{C}_a to denote $C_a(Y, L, W, Z; h_0, q_0)$ and $C_a(Y, L, W, Z; \hat{h}_0, \hat{q}_0)$ respectively for $a \in \{-1, 1\}$ when there is no confusion. As shown in Proposition 5.1, we have

$$V(d_3) = \mathbb{E}[C_1\mathbb{I}(d_3(L) = 1) + C_{-1}\mathbb{I}(d_3(L) = -1)] \triangleq V^{DR}(d_3),$$

for every $d_3 \in \mathcal{D}_3$. Then we can have

$$V(d_3^*) - V(\text{sign}(\hat{r}_3)) = V^{DR}(d_3^*) - V^{DR}(\text{sign}(\hat{r}_3)).$$

As stated in the main text, r^* is a minimizer of $\mathbb{E}[C_1\phi(r(L)) + C_{-1}\phi(-r(L))]$ and $d_3^* = \text{sign}(r^*)$ by Proposition 5.2. Define

$$r_{\rho_{4,n}} = \arg \min_{r \in \mathcal{R}_3} \{ \mathbb{E}[C_1\phi(r(L)) + C_{-1}\phi(-r(L))] + \rho_{4,n} \|r_3\|_{\mathcal{R}_3}^2 \}.$$

Then the corresponding approximation error is

$$\begin{aligned} \mathbb{A}(\rho_{4,n}) &= \mathbb{E}[C_1\phi(r_{\rho_{4,n}}(L)) + C_{-1}\phi(-r_{\rho_{4,n}}(L))] + \rho_{4,n} \|r_{\rho_{4,n}}\|_{\mathcal{R}_3}^2 \\ &\quad - \mathbb{E}[C_1\phi(r^*(L)) + C_{-1}\phi(-r^*(L))]. \end{aligned}$$

For notational convenience, we write \hat{r}_3^{DR} as \hat{r}_3 . By Proposition 5.3, we can show that

$$V^{DR}(d_3^*) - V^{DR}(\text{sign}(\hat{r}_3)) \leq R_\phi(\hat{r}_3) - R_\phi(r^*) \tag{31}$$

$$= R_\phi\left(\frac{1}{K} \sum_{k=1}^K \hat{r}_3^{(k)}\right) - R_\phi(r^*) \tag{32}$$

$$\leq \frac{1}{K} \sum_{k=1}^K R_\phi(\hat{r}_3^{(k)}) - R_\phi(r^*), \tag{33}$$

where the last inequality is implied by the convexity of $R_\phi(\bullet)$. Thus it suffices to consider $R_\phi(\hat{r}_3^{(k)}) -$

$R_\phi(r^*)$ for each $k = 1, \dots, K$. Observe that

$$\begin{aligned}
& R_\phi(\hat{r}_3^{(k)}) - R_\phi(r^*) \\
&= \mathbb{E} \left[C_1 \phi(\hat{r}_3^{(k)}) + C_{-1} \phi(-\hat{r}_3^{(k)}) \right] - \mathbb{E} \left[C_1 \phi(r^*(L)) + C_{-1} \phi(-r^*(L)) \right] \\
&\leq \rho_{4,n} \|r_{\rho_{4,n}}\|_{\mathcal{R}_3}^2 + \mathbb{E} \left[C_1 \phi(r_{\rho_{4,n}}(L)) + C_{-1} \phi(-r_{\rho_{4,n}}(L)) \right] - \mathbb{E} \left[C_1 \phi(r^*(L)) + C_{-1} \phi(-r^*(L)) \right] \\
&+ \mathbb{E} \left[C_1 \phi(\hat{r}_3^{(k)}) + C_{-1} \phi(-\hat{r}_3^{(k)}) \right] + \rho_{4,n} \|\hat{r}_3^{(k)}\|_{\mathcal{R}_3}^2 - \left\{ \rho_{4,n} \|r_{\rho_{4,n}}\|_{\mathcal{R}_3}^2 + \mathbb{E} \left[C_1 \phi(r_{\rho_{4,n}}(L)) + C_{-1} \phi(-r_{\rho_{4,n}}(L)) \right] \right\} \\
&= \mathbb{A}(\rho_{4,n}) + \sum_{a \in \mathcal{A}} \left\{ \mathbb{E} \left[C_a \phi(a \hat{r}_3^{(k)}) \right] - \mathbb{E} \left[C_a \phi(a r_{\rho_{4,n}}(L)) \right] \right\} + \rho_{4,n} \|\hat{r}_3^{(k)}\|_{\mathcal{R}_3}^2 - \rho_{4,n} \|r_{\rho_{4,n}}\|_{\mathcal{R}_3}^2.
\end{aligned}$$

In the following, we apply the empirical process theory to bound the second term on the right hand side of the inequality above. Let

$$\mathcal{G}_r \triangleq \left\{ \sum_{a \in \mathcal{A}} (C_a \phi(ar) - C_a \phi(ar_{\rho_{4,n}})) + \rho_{4,n} \|r\|_{\mathcal{R}_3}^2 - \rho_{4,n} \|r_{\rho_{4,n}}\|_{\mathcal{R}_3}^2 \mid \|r\|_{\mathcal{R}_3} \lesssim \rho_{4,n}^{-\frac{1}{2}} \right\}.$$

The reason why we only consider r that satisfies the above norm constraint is motivated by the following argument. By Assumptions 10 and 12, \hat{C}_a is uniformly bounded for every $a \in \mathcal{A}$. Then according to the optimization property, we can show that

$$\sum_{a \in \mathcal{A}} \mathbb{E}_n^{(-k)} \left[\hat{C}_a \phi(a \hat{r}_3^{(k)}) \right] + \rho_{4,n} \|\hat{r}_3^{(k)}\|_{\mathcal{R}_3}^2 \leq \sum_{a \in \mathcal{A}} \mathbb{E}_n^{(-k)} \left[\hat{C}_a \phi(0) \right],$$

which implies that $\rho_{4,n} \|\hat{r}_3^{(k)}\|_{\mathcal{R}_3}^2 \lesssim 1$. Based on this, we can further show that for any $g_r \in \mathcal{G}_r$,

$$\|g_r\|_\infty \lesssim \rho_{4,n}^{-\frac{1}{2}},$$

since $\rho_{4,n} \rightarrow 0$ and $\rho_{4,n} \leq 1$. The remaining proof consists of two steps. In the first step, we show

$$\mathbb{E}_n^{(-k)}(g_{\hat{r}_3^{(k)}}) \leq \varepsilon,$$

for some $\varepsilon > 0$ with a high probability. In the second step, we aim to show that

$$\sup_{g_r \in \mathcal{G}_r} \left| \mathbb{E}_n^{(-k)}(g_r) - \mathbb{E}(g_r) \right| \leq \delta,$$

with a high probability for some δ .

Step 1: This can be shown by first noting that

$$\begin{aligned} & \sum_{a \in \mathcal{A}} \mathbb{E}_n^{(-k)} \left(C_a \phi(a\hat{r}_3^{(k)}) - C_a \phi(ar_{\rho_{4,n}}) \right) + \rho_{4,n} \|\hat{r}_3^{(k)}\|_{\mathcal{R}_3}^2 - \rho_{4,n} \|r_{\rho_{4,n}}\|_{\mathcal{R}_3}^2 \\ & \leq \sum_{a \in \mathcal{A}} \mathbb{E}_n^{(-k)} \left(\hat{C}_a \phi(a\hat{r}_3^{(k)}) - \hat{C}_a \phi(ar_{\rho_{4,n}}) \right) + \rho_{4,n} \|\hat{r}_3^{(k)}\|_{\mathcal{R}_3}^2 - \rho_{4,n} \|r_{\rho_{4,n}}\|_{\mathcal{R}_3}^2 \\ & \quad + \sum_{a \in \mathcal{A}} \mathbb{E}_n^{(-k)} \left[\left(C_a - \hat{C}_a \right) \phi(a\hat{r}_3^{(k)}) - \left(C_a - \hat{C}_a \right) \phi(ar_{\rho_{4,n}}) \right] \\ & \leq \sum_{a \in \mathcal{A}} \mathbb{E}_n^{(-k)} \left[\left(C_a - \hat{C}_a \right) \phi(a\hat{r}_3^{(k)}) - \left(C_a - \hat{C}_a \right) \phi(ar_{\rho_{4,n}}) \right], \end{aligned}$$

where the last inequality is given by the optimization property. In the following, we bound the last term of the inequality above. It suffices to focus on $\mathbb{E}_n^{(-k)} \left[\left(C_a - \hat{C}_a \right) \phi(a\hat{r}_3) \right]$ for $a = 1$ while the other terms can be bounded similarly. It can be easily shown that

$$\begin{aligned} & \left| \mathbb{E}_n^{(-k)} \left[\left(C_1 - \hat{C}_1 \right) \phi(\hat{r}_3^{(k)}) \right] \right| \\ & \leq \left| \mathbb{E}_n^{(-k)} \left[\left(\mathbb{I}(A = 1)q_0(Z, 1, L) - \mathbb{I}(A = 1)\hat{q}_0^{(k)}(Z, 1, L) \right) \left(\hat{h}_0^{(k)}(W, 1, L) - h_0(W, 1, L) \right) \phi(\hat{r}_3^{(k)}) \right] \right| \\ & \quad + \left| \mathbb{E}_n^{(-k)} \left[\left(\mathbb{I}(A = 1)q_0(Z, 1, L) - \mathbb{I}(A = 1)\hat{q}_0^{(k)}(Z, 1, L) \right) (Y - h_0(W, 1, L)) \phi(\hat{r}_3^{(k)}) \right] \right| \\ & \quad + \left| \mathbb{E}_n^{(-k)} \left[\left(\mathbb{I}(A = 1)q_0(Z, 1, L) - 1 \right) \left(\hat{h}_0^{(k)}(W, 1, L) - h_0(W, 1, L) \right) \phi(\hat{r}_3^{(k)}) \right] \right| \\ & = (I) + (II) + (III). \end{aligned}$$

For (II), consider

$$\mathcal{G}_1 \triangleq \left\{ \left(\mathbb{I}(A = 1)q_0(Z, 1, L) - \mathbb{I}(A = 1)\hat{q}_0^{(k)}(Z, 1, L) \right) (Y - h_0(W, 1, L)) \phi(r) \mid \|r\|_{\mathcal{R}_3} \leq \rho_{4,n}^{-\frac{1}{2}} \right\}.$$

By the sample splitting and $\mathbb{E}[Y - h_0(W, 1, L) | Z, A = 1, L] = 0$, we can observe that $\mathbb{E}[g] = 0$ for any

$g \in \mathcal{G}_1$. In addition, the envelop function of \mathcal{G}_1 , defined as G_1 , is $C_0|\hat{q}_0^{(k)}(Z, 1, L) - q_0(Z, 1, L)| |Y - h_0(W, 1, L)| \rho_{4,n}^{-\frac{1}{2}}$. Therefore $\|G_1\|_{2,P} = C_0 n^{-\beta} \rho_{4,n}^{-\frac{1}{2}}$ by the error bound condition on $\hat{q}_0^{(k)}$ given in Assumption 12. By the entropy condition in Assumption 11 and Lipschitz property of ϕ , we can further show that

$$\sup_Q N(\mathcal{G}_1, Q, \varepsilon \|G_1\|_{2,Q}) \lesssim \left(\frac{1}{\varepsilon}\right)^v,$$

which implies that

$$J(1, \mathcal{G}_1, G_1) \triangleq \int_0^1 \sup_Q \sqrt{\log N(\mathcal{G}_1, Q, \varepsilon \|G_1\|_{2,Q})} \lesssim \sqrt{v}.$$

By leveraging the maximal inequality in the empirical process theory, we can show that

$$\mathbb{E} \sup_{g \in \mathcal{G}_1} |\mathbb{E}_n^{(-k)} g| \lesssim \sqrt{v} n^{-\frac{1}{2}} n^{-\beta} \rho_{4,n}^{-\frac{1}{2}}.$$

Then by Talagrand's inequality and assuming no issue of measurability (or simply applying Mcdiarmid's inequality), we can show with probability $1 - e^{-x}$,

$$\begin{aligned} (II) &\lesssim \mathbb{E} \sup_{g \in \mathcal{G}_1} |\mathbb{E}_n^{(-k)} g| + 2\sqrt{x} \sqrt{\frac{4\sqrt{v} n^{-\frac{1}{2}-\beta} \rho_{4,n}^{-1} + C_0 n^{-2\beta} \rho_{4,n}^{-1}}{n} + \frac{3x \rho_{4,n}^{-\frac{1}{2}}}{n}} \\ &\lesssim \max\{1, x\} \sqrt{v} n^{-\frac{1}{2}} n^{-\beta} \rho_{4,n}^{-\frac{1}{2}}. \end{aligned}$$

Similarly, we can show

$$(III) \lesssim \max\{1, x\} \sqrt{v} n^{-\frac{1}{2}} n^{-\alpha} \rho_{4,n}^{-\frac{1}{2}},$$

with probability at least $1 - e^{-x}$. In addition, we can bound (I) term by Cauchy-Schwarz inequality, i.e., with probability at least $1 - 2e^{-x}$,

$$\begin{aligned} (I) &\leq \left(\mathbb{E}_n^{(-k)} \left[q_0(Z, 1, L) - \hat{q}_0^{(k)}(Z, 1, L) \right]^2 \right)^{\frac{1}{2}} \times \left(\mathbb{E}_n^{(-k)} \left[h_0(W, 1, L) - \hat{h}_0^{(k)}(W, 1, L) \right]^2 \right)^{\frac{1}{2}} \rho_{4,n}^{-\frac{1}{2}} \\ &\lesssim \max\{1, x\} n^{-(\alpha+\beta)} \rho_{4,n}^{-\frac{1}{2}}. \end{aligned}$$

The last inequality is due to Bernstein's inequality, i.e.,

$$\mathbb{E}_n^{(-k)} \left[q_0(Z, 1, L) - \hat{q}_0^{(k)}(Z, 1, L) \right]^2 \lesssim n^{-2\beta} + n^{-\frac{1}{2}-\beta} \sqrt{2x} + \frac{x}{3n},$$

and

$$\mathbb{E}_n^{(-k)} \left[h_0(W, 1, L) - \hat{h}_0^{(k)}(W, 1, L) \right]^2 \lesssim n^{-2\beta} + n^{-\frac{1}{2}-\beta} \sqrt{2x} + \frac{x}{3n},$$

by the uniformly bounded assumption in Assumptions 10 and 12 and the error bound condition on nuisance function estimation in Assumption 12. Combining the results above together, we can show that with probability at least $1 - 3e^{-x}$,

$$\mathbb{E}_n^{(-k)} \left[\left(C_a - \hat{C}_a \right) \phi(a\hat{r}_3^{(k)}) \right] \lesssim \max\{1, x\} n^{-(\alpha+\beta)} \rho_{4,n}^{-\frac{1}{2}} + \max\{1, x\} \sqrt{vn}^{-\frac{1}{2}-\min\{\alpha,\beta\}} \rho_{4,n}^{-\frac{1}{2}}.$$

Similar result can be obtained by replacing $\hat{r}_3^{(k)}$ with $r_{\rho_{4,n}}$. So far, we have verified that

$$\mathbb{E}_n^{(-k)}(g_{\hat{r}_3^{(k)}}) \leq \varepsilon,$$

if $\varepsilon \geq C_0 \max\{1, x\} \left(n^{-(\alpha+\beta)} \rho_{4,n}^{-\frac{1}{2}} + n^{-\frac{1}{2}-\min\{\alpha,\beta\}} \rho_{4,n}^{-\frac{1}{2}} \right)$ with probability at least $1 - 12e^{-x}$.

Step 2: Again by applying Talagrand's inequality and maximal inequality, we can show that with probability at least $1 - e^{-x}$,

$$\sup_{g_r \in \mathcal{G}_r} \left| \mathbb{E}_n^{(-k)}(g_r) - \mathbb{E}(g_r) \right| \lesssim \max\{1, x\} \sqrt{v} \rho_{4,n}^{-\frac{1}{2}} n^{-\frac{1}{2}}.$$

Summarizing Step 1 and 2, we can show that with probability $1 - e^{-x}$,

$$\begin{aligned} & R_\phi(\hat{r}_3^{(k)}) - R_\phi(r^*) \\ & \lesssim \mathbb{A}(\rho_{4,n}) + \sum_{a \in \mathcal{A}} \left\{ \mathbb{E} \left[C_a \phi(a\hat{r}_3^{(k)}) \right] - \mathbb{E} \left[C_a \phi(ar_{\rho_{4,n}}(L)) \right] \right\} + \rho_{4,n} \|\hat{r}_3^{(k)}\|_{\mathcal{R}_3}^2 - \rho_{4,n} \|r_{\rho_{4,n}}\|_{\mathcal{R}_3}^2 \\ & \lesssim \mathbb{A}(\rho_{4,n}) + \sup_{g_r \in \mathcal{G}_r} \left| \mathbb{E}_n^{(-k)}(g_r) - \mathbb{E}(g_r) \right| + \mathbb{E}_n^{(-k)}(g_{\hat{r}_3^{(k)}}) \\ & \lesssim \max\{1, x\} \sqrt{v} \rho_{4,n}^{-\frac{1}{2}} n^{-\frac{1}{2}} + \max\{1, x\} n^{-(\alpha+\beta)} \rho_{4,n}^{-\frac{1}{2}} + \max\{1, x\} \sqrt{vn}^{-\frac{1}{2}-\min\{\alpha,\beta\}} \rho_{4,n}^{-\frac{1}{2}}, \end{aligned}$$

which concludes our proof.

C Computation Details

The implementation of the proximal policy learning involves selection of several tuning parameters and the cross-fitting procedure in Section 4.3. Data splitting will be used to implement the cross-fitting. We denote $I_a = \{i : A_i = a, i = 1, \dots, n\}$ for the indices of the treatment group ($A = 1$) and control group ($A = -1$). Let $I^{(1)}, \dots, I^{(K)}$ denote the indices of the randomly partitioned K folds of the indices $\{1, \dots, n\}$. Denote $I^{(-k)} = \{1, \dots, n\} \setminus I^{(k)}$, $k = 1, \dots, K$. Let $I_a^{(1)}, \dots, I_a^{(K)}$ denote the resulting indices of I_a after the random partition, $a = \pm 1$ and $I_a^{(-k)} = I_a \setminus I_a^{(k)}$, $k = 1, \dots, K$.

C.1 Estimation of Confounding Bridge Functions

Estimating h_0 . We introduce one more tuning parameter in (11). Consider a slightly modified optimization problem

$$\hat{h}_0 = \arg \min_{h \in \mathcal{H}} \left(\sup_{f \in \mathcal{F}} \left[\frac{1}{n} \sum_{i=1}^n \{Y_i - h(W_i, A_i, L_i)\} f(Z_i, A_i, L_i) - \lambda_1 (\|f\|_{\mathcal{F}}^2 + \xi \|f\|_{2,n}^2) \right] + \lambda_2 \|h\|_{\mathcal{H}}^2 \right), \quad (34)$$

where $\lambda_1 > 0$, $\lambda_2 > 0$ and $\xi > 0$ are tuning parameters.

If \mathcal{H} and \mathcal{F} are RKHSs equipped with kernels $K_{\mathcal{H}}$ and $K_{\mathcal{F}}$, and canonical RKHS norms $\|\bullet\|_{\mathcal{H}}$ and $\|\bullet\|_{\mathcal{F}}$ respectively, we can define the Gram matrices $\mathbf{K}_{\mathcal{H},n} = \left[K_{\mathcal{H}}([W_i, A_i, L_i], [W_j, A_j, L_j]) \right]_{i,j=1}^n$ and $\mathbf{K}_{\mathcal{F},n} = \left[K_{\mathcal{F}}([Z_i, A_i, L_i], [Z_j, A_j, L_j]) \right]_{i,j=1}^n$. Then the solution to (34) has the following closed form:

$$\hat{h}_0(w, a, l) = \sum_{i=1}^n \alpha_i K_{\mathcal{H}}([W_i, A_i, L_i], [w, a, l]), \quad \alpha = (\mathbf{K}_{\mathcal{H},n} \mathbf{M}_h \mathbf{K}_{\mathcal{H},n} + 4\lambda_1 \lambda_2 \mathbf{K}_{\mathcal{H},n})^\dagger \mathbf{K}_{\mathcal{H},n} \mathbf{M}_h Y,$$

where $\mathbf{M}_h = \mathbf{K}_{\mathcal{F},n}^{1/2} (\frac{\xi}{n} \mathbf{K}_{\mathcal{F},n} + \mathbf{I})^{-1} \mathbf{K}_{\mathcal{F},n}^{1/2}$, $Y = [Y_1, \dots, Y_n]^\top$, $\alpha = [\alpha_1, \dots, \alpha_n]^\top$ and A^\dagger is the Moore-Penrose pseudoinverse of A . This is a direct application of Propositions 9 and 10 in [Dikkala et al. \[2020\]](#).

In practice, we estimate $h(\bullet, a, \bullet)$ separately for $a = \pm 1$ by

$$\hat{h}_0(\bullet, a, \bullet) = \arg \min_{h \in \mathcal{H}} \left(\sup_{f \in \mathcal{F}} \left[\frac{1}{|I_a|} \sum_{i \in I_a} \{Y_i - h(W_i, a, L_i)\} f(Z_i, L_i) - \lambda_1 (\|f\|_{\mathcal{F}}^2 + \xi \|f\|_{2,n}^2) \right] + \lambda_2 \|h\|_{\mathcal{H}}^2 \right), \quad (35)$$

where \mathcal{H} is RKHS defined on $\mathcal{W} \times \mathcal{L}$ and \mathcal{F} is RKHS defined on $\mathcal{Z} \times \mathcal{L}$. The Gram matrices $\mathbf{K}_{\mathcal{H}, I_a} = \left[K_{\mathcal{H}}([W_i, L_i], [W_j, L_j]) \right]_{i,j \in I_a}$ and $\mathbf{K}_{\mathcal{F}, I_a} = \left[K_{\mathcal{F}}([Z_i, L_i], [Z_j, L_j]) \right]_{i,j \in I_a}$. Similarly, the solution to (35) has the following closed form expression: For each $a = \pm 1$,

$$\hat{h}_0(w, a, l) = \sum_{i \in I_a} \alpha_i K_{\mathcal{H}}([W_i, L_i], [w, l]), \quad \alpha = (\mathbf{K}_{\mathcal{H}, I_a} \mathbf{M}_{h, I_a} \mathbf{K}_{\mathcal{H}, I_a} + 4\lambda_1 \lambda_2 \mathbf{K}_{\mathcal{H}, I_a})^\dagger \mathbf{K}_{\mathcal{H}, I_a} \mathbf{M}_{h, I_a} Y,$$

where $\mathbf{M}_{h, I_a} = \mathbf{K}_{\mathcal{F}, I_a}^{-1/2} (\frac{\xi}{|I_a|} \mathbf{K}_{\mathcal{F}, I_a} + \mathbf{I})^{-1} \mathbf{K}_{\mathcal{F}, I_a}^{1/2}$, $Y = [Y_i]_{i \in I_a}^\top$, and $\alpha = [\alpha_i]_{i \in I_a}^\top$.

In the numerical studies, we equip \mathcal{H} and \mathcal{F} with Gaussian kernels $K_{\mathcal{H}}$ and $K_{\mathcal{F}}$ respectively. The bandwidth of $K_{\mathcal{F}}$ is selected using median heuristics, e.g., median of pairwise distance [Fukumizu et al., 2009]. The bandwidth of $K_{\mathcal{H}}$ and tuning parameters λ_1 and λ_2 are selected by cross-validation. See details in Algorithm 1.

Estimating q_0 . Similarly, we introduce one more tuning parameter in (13) and consider optimization problem for each $a = \pm 1$:

$$\hat{q}_0(\bullet, a, \bullet) = \arg \min_{q \in \mathcal{Q}} \left(\sup_{g \in \mathcal{G}} \left[\frac{1}{n} \sum_{i=1}^n \{\mathbb{I}(A_i = a) q(Z_i, a, L_i) - 1\} g(W_i, L_i) - \mu_1 (\|g\|_{\mathcal{G}}^2 + \zeta \|g\|_{2,n}^2) \right] + \mu_2 \|q\|_{\mathcal{Q}}^2 \right), \quad (36)$$

where $\mu_1 > 0$, $\mu_2 > 0$ and $\zeta > 0$ are tuning parameters.

Similar to the estimation of h_0 , suppose \mathcal{G} and \mathcal{Q} are the RKHSes of the kernels $K_{\mathcal{G}}$ and $K_{\mathcal{Q}}$, equipped with the canonical RKHS norms $\|\bullet\|_{\mathcal{G}}$ and $\|\bullet\|_{\mathcal{Q}}$. With corresponding Gram matrices $\mathbf{K}_{\mathcal{G}, n} = \left[K_{\mathcal{G}}([W_i, L_i], [W_j, L_j]) \right]_{i,j=1}^n$ and $\mathbf{K}_{\mathcal{Q}, n} = \left[K_{\mathcal{Q}}([Z_i, L_i], [Z_j, L_j]) \right]_{i,j=1}^n$, the solution to (36) is

$$\hat{q}_0(z, a, l) = \sum_{i=1}^n \alpha_i K_{\mathcal{Q}}([Z_i, L_i], [z, l]), \quad \alpha = \left(\mathring{\mathbf{K}}_{\mathcal{Q}, n}^\top \mathbf{M}_q \mathring{\mathbf{K}}_{\mathcal{Q}, n} + 4\mu_1 \mu_2 \mathbf{K}_{\mathcal{Q}, n} \right)^\dagger \mathring{\mathbf{K}}_{\mathcal{Q}, n}^\top \mathbf{M}_q \mathbf{1}_n,$$

where $\mathring{\mathbf{K}}_{\mathcal{Q},n} = \text{diag}\{\mathbb{I}(A_i = a)\}_{i=1}^n \mathbf{K}_{\mathcal{Q},n}$, $\mathbf{M}_q = \mathbf{K}_{\mathcal{G},n}^{1/2} (\frac{\zeta}{n} \mathbf{K}_{\mathcal{G},n} + \mathbf{I})^{-1} \mathbf{K}_{\mathcal{G},n}^{1/2}$ and $\mathbf{1}_n$ is column vector of 1's of length n . See details in Algorithm 2.

Selection of tuning parameters. There are several tuning parameters in the estimation of h_0 and q_0 . We accept the tricks and recommendation defaults by Dikkala et al. [2020] and their package `mliv`. The following parameters will be used to determine ξ , $\lambda_1 \lambda_2$, ζ and $\mu_1 \mu_2$. In particular, we define following two functions used in our tuning parameter selections.

$$\zeta(n) = 5/n^{0.4}. \quad (37)$$

$$\tau(s, n) = \frac{s}{2} \zeta^4(n). \quad (38)$$

More details can be found in Dikkala et al. [2020] and their package `mliv`. In all our numerical studies, RKHSs $\mathcal{F}, \mathcal{H}, \mathcal{G}, \mathcal{Q}$ are equipped with Gaussian kernels

$$K(x_1, x_2) = \exp\{\gamma \|x_1 - x_2\|_2^2\}. \quad (39)$$

The median heuristic bandwidth parameter $\gamma^{-1} = \text{median}\{\|x_i - x_j\|_2^2\}_{i < j \in I}$ for indices subset $I \subset \{1, \dots, n\}$ [Fukumizu et al., 2009]. Note that we only use median heuristic for $K_{\mathcal{F}}$ and $K_{\mathcal{G}}$.

Algorithm 1: Estimating $h_0(\bullet, a, \bullet)$, $a = \pm 1$

1 **Input:** Standardized data $\{(L_i, Z_i, W_i, Y_i)\}_{i \in I_a}$; Set bandwidth of \mathcal{F} by median heuristic.

2 Repeat for $k = 1, \dots, K$:

3 Repeat for bandwidth of \mathcal{H} by letting

$$\gamma_{\mathcal{H}}^{-1} \in \{p\text{-quantile of } \{\|[W_i, L_i] - [W_j, L_j]\|_2^2\}_{i < j \in I_a} : p = 0.1, \dots, 0.9\}$$

4 Repeat for s in a pre-specified collection of positive values:

$$5 \quad \xi^{(-k)} = 1/\zeta^2(|I_a^{(-k)}|), \lambda_1^{(-k)} \lambda_2^{(-k)} = \tau(s, |I_a^{(-k)}|), \xi^{(k)} = 1/\zeta^2(|I_a^{(k)}|).$$

6 Obtain $\hat{h}_0^{(-k)}(\bullet, a, \bullet)$ by (35) with standardized data of indices $I_a^{(-k)}$.

7 Calculate $r_i = Y_i - \hat{h}_0^{(-k)}(W_i, a, L_i)$, $i \in I_a^{(k)}$ and the loss $r^T M_{h, I_a^{(k)}} r / |I_a^{(k)}|^2$.

8 Calculate averaged loss along k . Find s^* and $\gamma_{\mathcal{H}}^*$ that minimize averaged loss.

9 **Output:** Calculate $\hat{h}_0(\bullet, a, \bullet)$ by (35) with $\xi = 1/\zeta^2(|I_a|)$, $\lambda_1 \lambda_2 = \tau(s^*, |I_a|)$ and $\gamma_{\mathcal{H}}^*$.

Algorithm 2: Estimating $q_0(\bullet, a, \bullet)$, $a = \pm 1$

- 1 **Input:** Standardized data $\{(L_i, Z_i, W_i, A_i)\}_{i=1}^n$; Set bandwidth of \mathcal{G} by median heuristic.
 - 2 Repeat for $k = 1, \dots, K$:
 - 3 Repeat for bandwidth of \mathcal{Q} by letting

$$\gamma_{\mathcal{Q}}^{-1} \in \{p\text{-quantile of } \{\| [Z_i, L_i] - [Z_j, L_j] \|_2^2\}_{i < j \in I_a} : p = 0.1, \dots, 0.9\}$$
 - 4 Repeat for s in a pre-specified collection of positive values:
 - 5 Let $n_a^{(k)} = |\{A_i = a : i \in I^{(k)}\}|$, $n_a^{(-k)} = |\{A_i = a : i \in I^{(-k)}\}|$.
 - 6 $\zeta^{(-k)} = 1/\zeta^2(n_a^{(-k)})$, $\mu_1^{(-k)} \mu_2^{(-k)} = \tau(s, n_a^{(-k)})$, $\zeta^{(k)} = 1/\zeta^2(n_a^{(k)})$.
 - 7 Obtain $\hat{q}_0^{(-k)}(\bullet, a, \bullet)$ by (36) with standardized data of indices $I^{(-k)}$.
 - 8 Calculate $r_i = 1 - \hat{q}_0^{(-k)}(Z_i, a, L_i)$, $i \in I^{(k)}$ and the loss $r^T M_{q, I^{(k)}} r / |I^{(k)}|^2$.
 - 9 Calculate averaged loss along k . Find s^* and $\gamma_{\mathcal{Q}}^*$ that minimize averaged loss.
 - 10 **Output:** Calculate $\hat{q}_0(\bullet, a, \bullet)$ by (36) with $\zeta = 1/\zeta^2(\sum_{i=1}^n \mathbb{I}(A_i = a))$,

$$\mu_1 \mu_2 = \tau(s^*, \sum_{i=1}^n \mathbb{I}(A_i = a))$$
 and $\gamma_{\mathcal{Q}}^*$.
-

C.2 Proximal Learning with RKHSs

In this subsection, we discuss algorithms of our proposed proximal learning using RKHSs. The algorithm of finding linear decision functions can be similarly obtained. We choose \mathcal{R}_i , $i = 1, 2$ to be RKHSs equipped with Gaussian kernels in (15) and (16). The bandwidth parameters of those Gaussian kernels are selected by a heuristic approach similar to Damodaran [2018]. Specifically, for a given dataset $\{(x_i, y_i, w_i)\}_{i=1}^n$ with class label $y_i \in \{-1, 1\}$ and sample weight $\{w_i\}_{i=1}^n$ such that $\sum_{i=1}^n w_i = 1$ and $w_i > 0, i = 1, \dots, n$, the empirical Hilbert-Schmidt Independence Criterion (HSIC) can be calculated by

$$\text{HSIC}(\{x_i, y_i, w_i\}_{i=1}^n; K_x, K_y) = n^{-2} \text{tr}(\mathbf{K}_x \mathbf{H} \mathbf{K}_y \mathbf{H}), \quad (40)$$

where $\mathbf{H} = \text{diag}(w) - ww^T$ with $w = (w_1, \dots, w_n)^T$, \mathbf{K}_x is the Gram matrix of Gaussian kernel K_x defined in (39) with bandwidth parameter γ and \mathbf{K}_y is the Gram matrix of target kernel K_y defined as

$$K_y(y_i, y_j) = \frac{\mathbb{I}(y_i = y_j)}{\#c_{y_i}}, \quad 1 \leq i, j \leq n,$$

where $\#c_{y_i} = \sum_{j=1}^n \mathbb{I}(y_j = y_i)$ [Section 5.2.2, Song et al., 2012]. Finally, the heuristic optimal bandwidth parameter γ is the one that maximizes the HSIC in (40).

In summary, details for implementing (15) are given in Algorithm 3. Algorithm 4 is given for (16) while Algorithm 5 is given for the maximum proximal learning (17). Details for the doubly robust proximal learning (22) with cross-fitting are provided in Algorithm 6. Note that cross-validation with cross-fitting requires another random splitting of training data. In Algorithm 6, we let $\{I^{(-k,\kappa)}\}_{\kappa=1}^K$ be the resulting indices of the random partition of $I^{(-k)}$ and denote $I^{(-k,-\kappa)} = I^{(-k)} \setminus I^{(-k,\kappa)}$, $k, \kappa = 1, \dots, K$.

Algorithm 3: Proximal Learning by (15)

- 1 **Input:** Standardized data $\{L_i, Z_i, W_i, A_i, Y_i\}_{i=1}^n$;
 - 2 Estimate \hat{h}_0 and calculate $\{\hat{\Delta}(W_i, L_i)\}_{i=1}^n$;
 - 3 Select bandwidth parameter $\gamma_{\mathcal{R}_1}$ of \mathcal{R}_1 by the HSIC heuristic approach.
 - 4 Repeat for $\rho_{1,n}$ in a pre-specified collection with size M :
 - 5 Repeat for $k = 1, \dots, K$:
 - 6 Estimate $\hat{h}_0^{(-k)}$ and calculate $\{\hat{\Delta}(W_i, L_i)\}_{i \in I^{(-k)}}$ with data of indices $I^{(-k)}$;
 - 7 Find $\hat{d}_1^{(-k)*}$ by (15) with \mathcal{R}_1 equipped with Gaussian kernel using bandwidth parameter $\gamma_{\mathcal{R}_1}$ and penalty coefficient $\rho_{1,n}$;
 - 8 Calculate empirical value $\hat{V}^{(k)}(\hat{d}_1^{(-k)*})$ with test data of indices $I^{(k)}$ by (4).
 - 9 Calculate averaged empirical value $K^{-1} \sum_{k=1}^K \hat{V}^{(k)}(\hat{d}_1^{(-k)*})$.
 - 10 Find $\rho_{1,n}^*$ that maximizes the average empirical value over M tuning parameters.
 - 11 **Output:** \hat{d}_1^* by (15) with \mathcal{R}_1 equipped with Gaussian kernel using bandwidth parameter $\gamma_{\mathcal{R}_1}$ and penalty coefficient $\rho_{1,n}^*$.
-

Algorithm 4: Proximal Learning by (16)

- 1 **Input:** Standardized data $\{L_i, Z_i, W_i, A_i, Y_i\}_{i=1}^n$;
 - 2 Estimate \hat{q}_0 and calculate $\{Y_i \hat{q}_0(Z_i, A_i, L_i)\}_{i=1}^n$;
 - 3 Select bandwidth parameter $\gamma_{\mathcal{R}_2}$ (16) by the HSIC heuristic approach.
 - 4 Repeat for $\rho_{2,n}$ in a pre-specified collection with size M :
 - 5 Repeat for $k = 1, \dots, K$:
 - 6 Estimate $\hat{q}_0^{(-k)}$ and calculate $\{Y_i \hat{q}_0^{(-k)}(Z_i, A_i, L_i)\}_{i \in I^{(-k)}}$ with data of indices $I^{(-k)}$;
 - 7 Find $\hat{d}_2^{(-k)*}$ by (16) with \mathcal{R}_2 equipped with Gaussian kernel using bandwidth parameter $\gamma_{\mathcal{R}_2}$ and penalty coefficient $\rho_{2,n}$;
 - 8 Calculate empirical value $\hat{V}^{(k)}(\hat{d}_2^{(-k)*})$ with test data of indices $I^{(k)}$ by (7).
 - 9 Calculate averaged empirical value $K^{-1} \sum_{k=1}^K \hat{V}^{(k)}(\hat{d}_2^{(-k)*})$.
 - 10 Find $\rho_{2,n}^*$ that maximizes the average empirical value among M tuning parameters.
 - 11 **Output:** \hat{d}_2^* by (16) with \mathcal{R}_2 equipped with Gaussian kernel using bandwidth parameter $\gamma_{\mathcal{R}_2}$ and penalty coefficient $\rho_{2,n}^*$.
-

Algorithm 5: Proximal Learning by (17)

- 1 **Input:** Standardized data $\{L_i, Z_i, W_i, A_i, Y_i\}_{i=1}^n$;
 - 2 Estimate \hat{h}_0 and calculate $\{\hat{\Delta}(W_i, L_i)\}_{i=1}^n$;
 - 3 Select bandwidth parameter $\gamma_{\mathcal{R}_1}$ of \mathcal{R}_1 by the HSIC heuristic approach.
 - 4 Estimate \hat{q}_0 and calculate $\{Y_i \hat{q}_0(Z_i, A_i, L_i)\}_{i=1}^n$;
 - 5 Select bandwidth parameter $\gamma_{\mathcal{R}_2}$ (16) by the HSIC heuristic approach.
 - 6 Do Lines 4-9 in Algorithm 3, Lines 4-9 in Algorithm 4.
 - 7 **if** $\max_{\rho_{1,n}} K^{-1} \sum_{k=1}^K \hat{V}^{(k)}(\hat{d}_1^{(-k)*}) \geq \max_{\rho_{2,n}} K^{-1} \sum_{k=1}^K \hat{V}^{(k)}(\hat{d}_2^{(-k)*})$, **then**
 - 8 **Output:** \hat{d}_1^* by Lines 10-11 in Algorithm 3
 - 9 **else:**
 - 10 **Output:** \hat{d}_2^* by Lines 10-11 in Algorithm 4
 - 11 **end if**
-

Algorithm 6: Proximal Learning for doubly robust ITR (22)

- 1 **Input:** Standardized data $\{L_i, Z_i, W_i, A_i, Y_i\}_{i=1}^n$;
 - 2 Estimate \hat{h}_0, \hat{q}_0 and calculate $\{C_a(Y_i, L_i, W_i, Z_i; \hat{h}_0, \hat{q}_0), a = \pm 1\}_{i=1}^n$ by (19);
 - 3 Select bandwidth parameter $\gamma_{\mathcal{R}_3}$ (22) by the HSIC heuristic approach.
 - 4 Repeat for $\rho_{4,n}$ in a pre-specified collection with size M :
 - 5 Repeat for $k = 1, \dots, K$:
 - 6 Repeat for $\kappa = 1, \dots, K$:
 - 7 Estimate $\hat{h}_0^{(-k, \kappa)}, \hat{q}_0^{(-k, \kappa)}$ with data of indices $I^{(-k, \kappa)}$;
 - 8 Obtain $\{C_a(Y_i, L_i, W_i, Z_i; \hat{h}_0^{(-k, \kappa)}, \hat{q}_0^{(-k, \kappa)}), a = \pm 1\}_{i \in I^{(-k, -\kappa)}}$ by (19) with data of indices $I^{(-k, -\kappa)}$;
 - 9 Find $\hat{r}_3^{DR, (-k, -\kappa)}$ by (22) with \mathcal{R}_3 equipped with Gaussian kernel using bandwidth parameter $\gamma_{\mathcal{R}_3}$ and penalty coefficient $\rho_{4,n}$.
 - 10 Define aggregated estimator $\hat{d}_3^{DR, (-k)} = \text{sign}(K^{-1} \sum_{\kappa=1}^K \hat{r}_3^{DR, (-k, -\kappa)})$.
 - 11 Calculate empirical value $\hat{V}^{(k)}(\hat{d}_3^{DR, (-k)})$ with test data of indices $I^{(k)}$ by (21).
 - 12 Calculate averaged empirical value $K^{-1} \sum_{k=1}^K \hat{V}^{(k)}(\hat{d}_3^{DR, (-k)})$.
 - 13 Find $\rho_{4,n}^*$ that maximizes averaged empirical value among M tuning parameters.
 - 14 Repeat for $k = 1, \dots, K$:
 - 15 Estimate $\hat{h}_0^{(k)}, \hat{q}_0^{(k)}$ with data of indices $I^{(k)}$;
 - 16 Obtain $\{C_a(Y_i, L_i, W_i, Z_i; \hat{h}_0^{(k)}, \hat{q}_0^{(k)}), a = \pm 1\}_{i \in I^{(-k)}}$ by (19) with data of indices $I^{(-k)}$;
 - 17 Find $\hat{r}_3^{DR, (-k)}$ by (22) with \mathcal{R}_3 equipped with Gaussian kernel using bandwidth parameter $\gamma_{\mathcal{R}_3}$ and penalty coefficient $\rho_{4,n}^*$.
 - 18 **Output:** Aggregated estimator $\hat{d}_3^{DR} = \text{sign}(K^{-1} \sum_{k=1}^K \hat{r}_3^{DR, (-k)})$.
-

D Choices of Parameters for Simulation Data Generation

D.1 Data Generation of (L, W, A, Z, U)

Step 1. We consider generating data (L, W, A, Z, U) such that for $a = -1, 1$,

$$\frac{1}{\Pr(A = a | U, L)} = \int q_0(z, a, L) dF(z | U, a, L).$$

Let

$$q_0(Z, A, L) = 1 + \exp\{A(t_0 + t_z Z + t_a \mathbb{I}(A = 1) + t_l L)\}.$$

Therefore, we have that

$$\frac{1}{\Pr(A | U, L)} = 1 + \exp\{A(t_0 + t_a \mathbb{I}(A = 1) + t_l L)\} \int \exp\{At_z z\} dF(z | U, A, L)$$

Suppose that

$$Z | U, A, L \sim N(\theta_0, \theta_a \mathbb{I}(A = 1) + \theta_u U + \theta_l L, \sigma_{z|u,a,l}^2), \quad (41)$$

so that

$$\frac{1}{\Pr(A | U, L)} = 1 + \exp\left\{A(t_0 + t_a \mathbb{I}(A = 1) + t_l L) + At_z(\theta_0 + \theta_a \mathbb{I}(A = 1) + \theta_u U + \theta_l L) + \frac{t_z^2 \sigma_{z|u,a,l}^2}{2}\right\}. \quad (42)$$

We require that $\Pr(A = 1 | U, L) + \Pr(A = -1 | U, L) = 1$. Since $\Pr(A = a | U, L)$ is in the form of expit, we only need

$$\begin{aligned} & t_0 + t_a + t_l L + t_z(\theta_0 + \theta_a + \theta_u U + \theta_l L) + \frac{t_z^2 \sigma_{z|u,a,l}^2}{2} \\ &= t_0 + t_l L + t_z(\theta_0 + \theta_u U + \theta_l L) - \frac{t_z^2 \sigma_{z|u,a,l}^2}{2}, \end{aligned}$$

which implies that

$$t_a = -t_z^2 \sigma_{z|u,a,l}^2 - t_z \theta_a.$$

Therefore,

$$q_0(Z, A, L) = 1 + \exp \left\{ A[t_0 + t_z Z + t_l L - t_z^2 \sigma_z^2|_{u,a,l} \mathbb{I}(A=1) - t_z \theta_a \mathbb{I}(A=1)] \right\}.$$

Step 2. Let

$$(Z, W, U) | A, L \sim N \left(\begin{bmatrix} \alpha_0 + \alpha_a \mathbb{I}(A=1) + \alpha_l L \\ \mu_0 + \mu_a \mathbb{I}(A=1) + \mu_l L \\ \kappa_0 + \kappa_a \mathbb{I}(A=1) + \kappa_l L \end{bmatrix}, \begin{bmatrix} \sigma_z^2 & \sigma_{zw} & \sigma_{zu} \\ \sigma_{zw} & \sigma_w^2 & \sigma_{wu} \\ \sigma_{zu} & \sigma_{wu} & \sigma_u^2 \end{bmatrix} \right)$$

Therefore,

$$\mathbb{E}(Z | U, A, L) = \alpha_0 + \alpha_a + \alpha_l L + \frac{\sigma_{zu}}{\sigma_u^2} (U - \kappa_0 - \kappa_a \mathbb{I}(A=1) - \kappa_l L).$$

Compare it with (41), we have

$$\theta_0 = \alpha_0 - \frac{\sigma_{zu}}{\sigma_u^2} \kappa_0, \quad \theta_a = \alpha_a - \frac{\sigma_{zu}}{\sigma_u^2} \kappa_a, \quad \theta_l = \alpha_l - \frac{\sigma_{zu}}{\sigma_u^2} \kappa_l, \quad \theta_u = \frac{\sigma_{zu}}{\sigma_u^2}.$$

In addition, we impose

$$W \perp\!\!\!\perp (A, Z) | U, L.$$

The independence implies that $W | U, A, Z, L$ follows

$$N \left(\begin{bmatrix} \mu_0 + \mu_a \mathbb{I}(A=1) + \mu_l L + \Sigma_{w(u,l)} \Sigma_{u,z}^{-1} [U - \kappa_0 - \kappa_a \mathbb{I}(A=1) - \kappa_l L] \\ Z - \alpha_0 - \alpha_a \mathbb{I}(A=1) - \alpha_l L \end{bmatrix}, \sigma_w^2 - \Sigma_{w(u,l)} \Sigma_{u,z}^{-1} \Sigma_{w(u,l)}^\top \right),$$

where $\Sigma_{w(u,z)} = \begin{bmatrix} \sigma_{wu} & \sigma_{wz} \end{bmatrix}$, $\Sigma_{u,z} = \begin{bmatrix} \sigma_u^2 & \sigma_{zu} \\ \sigma_{zu} & \sigma_z^2 \end{bmatrix}$, such that

$$\mathbb{E}(W | U, A, Z, L) = \mathbb{E}(W | U, A, L) = \mu_0 + \mu_a \mathbb{I}(A=1) + \mu_l L + \frac{\sigma_{wu}}{\sigma_u^2} \{U - (\kappa_0 + \kappa_a \mathbb{I}(A=1) - \kappa_l L)\}$$

does not depend on A and Z . Therefore

$$\frac{\sigma_{wz}\sigma_u^2 - \sigma_{wu}\sigma_{zu}}{\sigma_z^2\sigma_u^2 - \sigma_{zu}^2} = 0,$$

and

$$\mu_a = \frac{\sigma_{wu}}{\sigma_u^2} \kappa_a.$$

Step 3.1. Notice that $\Pr(A = a | U, L) = \Pr(A = a | U, W, L)$, their log odds ratio with respect to U must be the same, i.e.,

$$\begin{aligned} & \underbrace{\log \frac{\Pr(A = 1 | U = u, L) / \Pr(A = -1 | U = u, L)}{\Pr(A = 1 | U = 0, L) / \Pr(A = -1 | U = 0, L)}}_{\text{logOR1}} \\ &= \log \underbrace{\frac{\Pr(A = 1 | U = u, W, L) / \Pr(A = -1 | U = u, W, L)}{\Pr(A = 1 | U = 0, W, L) / \Pr(A = -1 | U = 0, W, L)}}_{\text{logOR2}}. \end{aligned}$$

By the expit property of (42),

$$\text{logOR1} = -t_z \theta_u u.$$

Moreover,

$$\Pr(A = a | U, W, L) = \frac{\Pr(U | A = a, W, L) \Pr(A = a, W, L)}{\Pr(U, W, L)}$$

implies that

$$\begin{aligned} & \text{logOR2} \\ &= \log \frac{\Pr(A = 1 | U = u, W, L) / \Pr(A = -1 | U = u, W, L)}{\Pr(A = 1 | U = 0, W, L) / \Pr(A = -1 | U = 0, W, L)} \\ &= \log \frac{\Pr(U = u | A = 1, W, L) / \Pr(U = u | A = -1, W, L)}{\Pr(U = 0 | A = 1, W, L) / \Pr(U = 0 | A = -1, W, L)}. \end{aligned}$$

Notice that $U | A, W, L \sim N\left(\mathbb{E}(U | A, W, L), \sigma_{u|w,a,l}^2 := \sigma_{u|w,l}^2\right)$ where the variance does not depend on $a = -1$ or $a = 1$, so

$$\log \frac{\Pr(U = u | A = 1, W, L)}{\Pr(U = u | A = -1, W, L)} = -\frac{1}{2\sigma_{u|w,l}^2} \left[-2u \{ \mathbb{E}(U | W, A = 1, L) - \mathbb{E}(U | W, A = -1, L) \} \right. \\ \left. + \mathbb{E}^2(U | W, A = 1, L) - \mathbb{E}^2(U | W, A = -1, L) \right].$$

Therefore,

$$\log \text{OR2} = \frac{\mathbb{E}(U | W, A = 1, L) - \mathbb{E}(U | W, A = -1, L)}{\sigma_{u|w,l}^2} u = \frac{\kappa_a - \sigma_{wu}\mu_a/\sigma_w^2}{\sigma_{u|w,l}^2} u.$$

Finally, we have that

$$-t_z \theta_u = \frac{\kappa_a - \sigma_{wu}\mu_a/\sigma_w^2}{\sigma_{u|w,l}^2}.$$

Step 3.2. To find the parameters in q_0 , we require the constraint

$$\Pr(A = -1 | W, L) = \Pr(A = 1 | W, L) = 1.$$

Recall that since $\sigma_{u|w,a,l}^2 = \sigma_{u|w,l}^2$,

$$\frac{1}{\Pr(A = a | W, L)} = \int \frac{1}{\Pr(A = a | U, W, L)} dF(U | W, A = a, L) \\ = 1 + \exp \left\{ a[t_0 + t_a \mathbb{I}(a = 1) + t_l L + t_z(\theta_0 + \theta_a + \theta_l L)] + \frac{t_z^2 \sigma_{z|u,a,l}^2}{2} \right\} \\ \times \int \exp \{ at_z \theta_u U \} dF(U | W, A = a, L) \\ = 1 + \exp \left\{ a[t_0 + t_a \mathbb{I}(a = 1) + t_l L + t_z(\theta_0 + \theta_a + \theta_l L)] + \frac{t_z^2 \sigma_{z|u,a,l}^2}{2} \right\} \\ \times \exp \left\{ at_z \theta_u \mathbb{E}(U | W, A = a, L) + \sigma_{u|w,l}^2 \frac{t_z^2 \theta_u^2}{2} \right\}.$$

Similarly, we require that

$$\begin{aligned}
& t_0 + t_a + t_l L + t_z(\theta_0 + \theta_a + \theta_l L) + \frac{t_z^2 \sigma_{z|u,a,l}^2}{2} \\
& + t_z \theta_u \{ \mathbb{E}(U | W, A = 1, L) - \mathbb{E}(U | W, A = -1, L) \} + \sigma_{u|w,l}^2 \frac{t_z^2 \theta_u^2}{2} \\
& = t_0 + t_l L + t_z(\theta_0 + \theta_l L) - \frac{t_z^2 \sigma_{z|u,a,l}^2}{2} - \sigma_{u|w,l}^2 \frac{t_z^2 \theta_u^2}{2},
\end{aligned}$$

which holds because

$$\mathbb{E}(U | W, A = 1, L) - \mathbb{E}(U | W, A = -1, L) = -t_z \theta_u \sigma_{u|w,l}^2,$$

as shown in Step 3.1 and

$$t_a = -t_z^2 \sigma_{z|u,a,l}^2 - t_z \theta_a,$$

required in Step 1.

Step 4. Finally, we require that

$$\Pr(A = 1 | U, L) + \Pr(A = -1 | U, L) = 1.$$

Notice that

$$\begin{aligned}
& \frac{1}{\Pr(A = a | L)} \\
&= \int \frac{1}{\Pr(A | U, L)} dF(U | A = a, L) \\
&= 1 + \exp \left\{ a [t_0 + t_a \mathbb{I}(a = 1) + t_l L + t_z(\theta_0 + \theta_a \mathbb{I}(a = 1) + \theta_l L)] + \frac{t_z^2 \sigma_z^2 |_{u,a,l}}{2} \right\} \\
&\quad \times \int \exp \{ at_z \theta_u U \} dF(U | A = a, L) \\
&= 1 + \exp \left\{ a [t_0 + t_a \mathbb{I}(a = 1) + t_l L + t_z(\theta_0 + \theta_a \mathbb{I}(a = 1) + \theta_l L)] + \frac{t_z^2 \sigma_z^2 |_{u,a,l}}{2} \right\} \\
&\quad \times \exp \left\{ at_z \theta_u \mathbb{E}(U | A = a, L) + \sigma_{u|a,l}^2 \frac{t_z^2 \theta_u^2}{2} \right\} \\
&= 1 + \exp \left\{ a [t_0 + t_a \mathbb{I}(a = 1) + t_l L + t_z(\theta_0 + \theta_a \mathbb{I}(a = 1) + \theta_l L)] + \frac{t_z^2 \sigma_z^2 |_{u,a,l}}{2} \right\} \\
&\quad \times \exp \left\{ at_z \theta_u (\kappa_0 + \kappa_a \mathbb{I}(a = 1) + \kappa_l L) + \sigma_{u|a,l}^2 \frac{t_z^2 \theta_u^2}{2} \right\}.
\end{aligned}$$

Thus, $A | L$ is generated by

$$\begin{aligned}
\frac{1}{\Pr(A = 1 | L)} &= 1 + \exp \left\{ t_0 + t_a + t_l L + t_z(\theta_0 + \theta_a + \theta_l L) + \frac{t_z^2 (1 - \frac{\sigma_{zu}^2}{\sigma_z^2 \sigma_u^2}) \sigma_z^2}{2} \right\} \\
&\quad \times \exp \left\{ t_z \theta_u (\kappa_0 + \kappa_a + \kappa_l L) + \sigma_u^2 \frac{t_z^2 \theta_u^2}{2} \right\}.
\end{aligned}$$

Here we provide a summary of the constraints of data generation:

$$\begin{aligned}
t_a &= -t_z^2 \sigma_z^2 |_{u,a,l} - t_z \theta_a = -t_z^2 (1 - \frac{\sigma_{zu}^2}{\sigma_z^2 \sigma_u^2}) \sigma_z^2 - t_z \theta_a, \\
\sigma_{wz} \sigma_u^2 - \sigma_{wu} \sigma_{zu} &= 0, \\
\mu_a \sigma_u^2 &= \sigma_{wu} \kappa_a, \\
-\theta_u t_z (1 - \frac{\sigma_{uw}^2}{\sigma_u^2 \sigma_w^2}) \sigma_u^2 &= -\theta_u \sigma_{u|w,a,l}^2 t_z = \kappa_a - \sigma_{wu} \mu_a / \sigma_w^2.
\end{aligned}$$

We used following setting for the generation of (L, W, A, Z, U) :

- $\alpha_0 = 0.25, \alpha_a = 0.25, \alpha_l = [0.25, 0.25]$;
- $\mu_0 = 0.25, \mu_a = 0.125, \mu_l = [0.25, 0.25]$;
- $\kappa_0 = 0.25, \kappa_a = 0.25, \kappa_l = [0.25, 0.25]$;
- $\Sigma = \begin{bmatrix} 1 & 0.25 & 0.5 \\ 0.25 & 1 & 0.5 \\ 0.5 & 0.5 & 1 \end{bmatrix}$

Then the steps above are compatible with the model of q_0 :

$$q_0(Z, A, L) = 1 + \exp \{A(t_0 + t_z Z + t_a \mathbb{I}(A = 1) + t_l L)\},$$

where $t_0 = 0.25, t_z = -0.5$, and $t_a = -0.125$,

D.2 Data Generation of $Y \mid L, W, A, Z, U$

We generate response Y given L, W, A, Z, U such that $Z \perp\!\!\!\perp Y \mid U, A, L$ and Assumption 7 holds, i.e., for $a = -1, 1$,

$$\mathbb{E}(Y \mid U, a, L) = \int h_0(w, a, L) dF(w \mid U, L),$$

which we impose by letting

$$\begin{aligned} \mathbb{E}(Y \mid W, U, A, Z, L) &= \mathbb{E}(Y \mid U, A, Z, L) + \omega \{W - \mathbb{E}(W \mid U, A, Z, L)\} \\ &= \mathbb{E}(Y \mid U, A, L) + \omega \{W - \mathbb{E}(W \mid U, L)\} \text{ since } W \perp\!\!\!\perp (A, Z) \mid U, L. \end{aligned} \quad (43)$$

1. When $\mathbb{E}(Y \mid W, U, A, Z, L)$ is linear of L , let

$$h_0(W, A, L) = c_0 + c_1 \mathbb{I}(A = 1) + c_2 W + c_3 L + \mathbb{I}(A = 1)(c_4 W + c_5 L).$$

Then by (43),

$$\begin{aligned}
\mathbb{E}(Y \mid W, U, A, Z, L) &= \int h_0(w, A, L) dF(w \mid U, L) - \omega \mathbb{E}(W \mid U, L) + \omega W \\
&= c_0 + c_1 \mathbb{I}(A = 1) + c_3 L + c_5 \mathbb{I}(A = 1) L + \omega W \\
&\quad + (c_2 + c_4 \mathbb{I}(A = 1) - \omega) \mathbb{E}(W \mid U, L) \\
&= c_0 + c_1 \mathbb{I}(A = 1) + c_3 L + c_5 \mathbb{I}(A = 1) L + \omega W \\
&\quad + (c_2 + c_4 \mathbb{I}(A = 1) - \omega) \left\{ \mu_0 + \mu_l L + \frac{\sigma_{wu}}{\sigma_u^2} (U - \kappa_0 - \kappa_l L) \right\}.
\end{aligned}$$

- When $c_4 = 0$, $h_0(W, A = 1, L) - h_0(W, A = -1, L)$ only depends on L .

The global optimal ITR is $d^*(L, U) = \text{sign}(\mathbb{E}[Y \mid L, U, A = 1] - \mathbb{E}[Y \mid L, U, A = -1])$.

$$\begin{aligned}
&\mathbb{E}[Y \mid L, U, A = 1] - \mathbb{E}[Y \mid L, U, A = -1] \\
&= \mathbb{E} \{ \mathbb{E}[Y \mid W, U, A, Z, L] \mid L, U, A = 1 \} - \mathbb{E} \{ \mathbb{E}[Y \mid W, U, A, Z, L] \mid L, U, A = -1 \} \\
&= c_1 + c_5 L + \omega \underbrace{\{ \mathbb{E}(W \mid L, U, A = 1) - \mathbb{E}(W \mid L, U, A = -1) \}}_{=0 \text{ since } W \perp\!\!\!\perp A \mid L, U} \\
&\quad + c_4 \left\{ \mu_0 + \mu_l L + \frac{\sigma_{wu}}{\sigma_u^2} (U - \kappa_0 - \kappa_l L) \right\} \\
&= c_1 + c_5 L + c_4 \left\{ \mu_0 + \mu_l L + \frac{\sigma_{wu}}{\sigma_u^2} (U - \kappa_0 - \kappa_l L) \right\}.
\end{aligned}$$

The optimal ITR within \mathcal{D}_3 is

$$\begin{aligned}
d_3^*(L) &= \text{sign}(\mathbb{E}[h_0(W, A = 1, L) \mid L] - \mathbb{E}[h_0(W, A = -1, L) \mid L]) \\
&= c_1 + c_4 \mathbb{E}(W \mid L) + c_5 L \\
&= c_1 + c_4 \mathbb{E}[\mathbb{E}(W \mid L, A) \mid L] + c_5 L \\
&= c_1 + c_4 [(\mu_0 + \mu_a + \mu_l L) P(A = 1 \mid L) + (\mu_0 + \mu_l L) P(A = -1 \mid L)] + c_5 L \\
&= c_1 + c_4 [\mu_0 + \mu_l L + \mu_a P(A = 1 \mid L)] + c_5 L.
\end{aligned}$$

2. When $\mathbb{E}(Y \mid W, U, A, Z, L)$ is nonlinear of L , let

$$h_0(W, A, L) = c_0 + c_1(A) + c_2W + c_3(L) + \mathbb{I}(A = 1) \{c_4W + c_5(L) + Wc_6(L)\}.$$

Then by (43),

$$\begin{aligned} \mathbb{E}(Y \mid W, U, A, Z, L) &= \int h_0(w, A, L) dF(w \mid U, L) - \omega \mathbb{E}(W \mid U, L) + \omega W \\ &= c_0 + c_1(A) + c_3(L) + \mathbb{I}(A = 1)c_5(L) \\ &\quad + \{c_2 + c_4\mathbb{I}(A = 1) + Ac_6(L) - \omega\} \mathbb{E}(W \mid U, L) + \omega W \\ &= c_0 + c_1(A) + c_3(L) + \mathbb{I}(A = 1)c_5(L) + \omega W \\ &\quad + \{c_2 + c_4\mathbb{I}(A = 1) + Ac_6(L) - \omega\} \left\{ \mu_0 + \mu_l L + \frac{\sigma_{wu}}{\sigma_u^2} (U - \kappa_0 - \kappa_l L) \right\}. \end{aligned}$$

- When $c_4, c_6(\cdot) = 0$, $h_0(W, A = 1, L) - h_0(W, A = -1, L)$ only depends on L .

The global optimal ITR is $d^*(L, U) = \text{sign}(\mathbb{E}[Y \mid L, U, A = 1] - \mathbb{E}[Y \mid L, U, A = -1])$.

$$\begin{aligned} &\mathbb{E}[Y \mid L, U, A = 1] - \mathbb{E}[Y \mid L, U, A = -1] \\ &= \mathbb{E} \{ \mathbb{E}[Y \mid W, U, A, Z, L] \mid L, U, A = 1 \} - \mathbb{E} \{ \mathbb{E}[Y \mid W, U, A, Z, L] \mid L, U, A = -1 \} \\ &= c_1(1) - c_1(0) + c_5(L) + \omega \underbrace{\{ \mathbb{E}(W \mid L, U, A = 1) - \mathbb{E}(W \mid L, U, A = -1) \}}_{=0 \text{ since } W \perp\!\!\!\perp A \mid L, U} \\ &\quad + [c_4 + c_6(L)] \left\{ \mu_0 + \mu_l L + \frac{\sigma_{wu}}{\sigma_u^2} (U - \kappa_0 - \kappa_l L) \right\} \\ &= c_1(1) - c_1(0) + c_5(L) + [c_4 + c_6(L)] \left\{ \mu_0 + \mu_l L + \frac{\sigma_{wu}}{\sigma_u^2} (U - \kappa_0 - \kappa_l L) \right\}. \end{aligned}$$

The optimal ITR within \mathcal{D}_3 is

$$\begin{aligned}
d_3^*(L) &= \text{sign}(\mathbb{E}[h_0(W, A = 1, L) \mid L] - \mathbb{E}[h_0(W, A = -1, L) \mid L]) \\
&= c_1(1) - c_1(-1) + c_5(L) + (c_4 + c_6(L))\mathbb{E}(W \mid L) \\
&= c_1(1) - c_1(-1) + c_5(L) + (c_4 + c_6(L))\mathbb{E}[\mathbb{E}(W \mid L, A) \mid L] \\
&= c_1(1) - c_1(-1) + c_5(L) + (c_4 + c_6(L)) \{ \mu_0 + \mu_l L + \mu_a P(A = 1 \mid L) \}.
\end{aligned}$$

E Additional Simulation Results

In addition to the results in Section 6.2, for L1 and L2, we also compare our proposed optimal ITR estimators with $\text{dEARL}(L, W)$, $\text{dEARL}(L, Z)$ and $\text{dEARL}(L, Z, W)$. Similar to $\text{dEARL}(L)$, we use all observed variables (L, W, Z) to construct tree-based nonparametric main effect models and propensity score models, then fit the regime in terms of (L, W) , (L, Z) and (L, Z, W) , respectively.

Figures 8, 9 refer to L1 and L2 scenarios with sample size $n = 2,000$ and $5,000$. Generally, our methods perform better than EARL in all kinds of regime in terms of (L, W) , (L, Z) , (L, Z, W) or L , when $n = 5,000$. For $n = 2,000$, $\text{d2}(L, W)$ is no better than $\text{dEARL}(L, W)$ in both Figure 8 (a) and Figure 9 (a). This demonstrates the difficulty of estimating q_0 for small sample.

Figure 10 refers to our N1 and N2 scenarios with sample size $n = 2,000$. Similar interpretations can be obtained as those in the main text.

In the following, we also study the statistical inference related to $V(d_3)$ for $d_3 \in \mathcal{D}_3$. Table 6 refers to the inference results of $V(d_3)$ at $d_3 = d_3^*$ for all simulation scenarios. The point estimates of $V(d_3^*)$ were calculated by (21) in the main text. The 95% confidence intervals of $V(d_3)$ were constructed according to Theorem 4.1. For each scenario L1, L2, N1, N2 and sample size $n = 2,000, 5000$, we ran 1,000 simulations to obtain the mean squared error (MSE), averaged length of CIs (Avg. CI Length) and coverage rate. Results shown in Table 6 indicate satisfactory performances of using doubly robust estimator in evaluating $V(d_3)$.

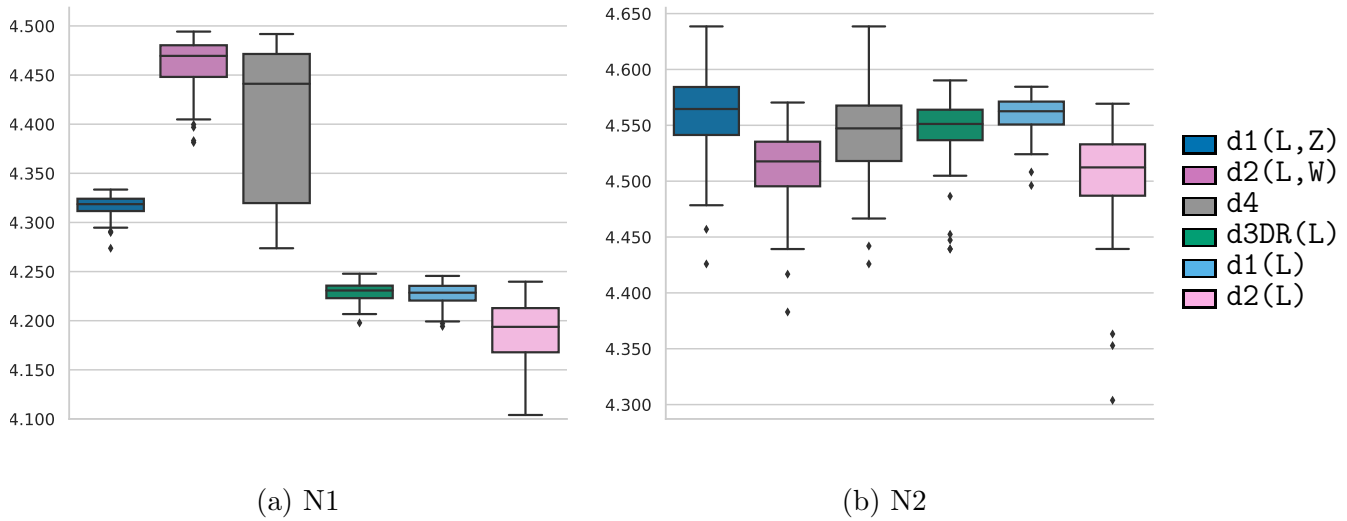


Figure 10: Boxplots of values for Scenario N1 and N2 with sample size $n = 2,000$.

Table 6: Inferences of efficient influence function at d_3^* .

Scenario	n	$V(d_3^*)$	MSE	Avg. CI Length	Coverage Rate
L1	2,000	6.258	0.0191	0.628	97.6%
L1	5,000	6.258	0.0108	0.425	96.2%
L2	2,000	6.203	0.0183	0.615	98.3%
L2	5,000	6.203	0.0104	0.416	96.1%
N1	2,000	4.244	0.0067	0.332	95.3%
N1	5,000	4.244	0.0031	0.218	95.8%
N2	2,000	4.602	0.0081	0.378	96.3%
N2	5,000	4.602	0.0043	0.247	94.0%

F Additional Results of Real Data Application

All coefficients of the five optimal linear ITR estimates in comparison are given in Table 7 and illustrated in Figure 11.

Table 7: All coefficients of the five optimal linear ITR estimates.

Covariate	d1(L)	d1(L,Z)	d2(L,W)	d2(L)	d3DR(L)
intercept	-1.215	-1.222	-0.204	-0.258	-0.722
cardiohx	-0.109	-0.085	0.033	0.007	0.045

chfhx	0.391	0.348	0.059	0.055	0.041
dementhx	0.001	-0.021	-0.171	-0.167	-0.003
psychhx	-0.112	-0.079	-0.188	-0.200	0.007
chrpulhx	0.046	0.061	-0.023	-0.042	-0.038
renalhx	0.612	0.579	0.111	0.096	0.061
liverhx	0.447	0.451	-0.025	-0.056	0.008
gibledhx	-0.343	-0.328	-0.511	-0.490	-0.065
malighx	-0.797	-0.622	0.170	0.181	0.017
immunhx	0.296	0.296	0.217	0.226	0.132
transhx	0.827	0.802	0.486	0.488	0.136
amihx	0.031	-0.019	0.388	0.333	0.008
age	-0.421	-0.413	-0.079	-0.065	-0.043
sex	-0.459	-0.455	-0.112	-0.105	-0.109
edu	0.209	0.211	0.050	0.039	0.046
surv2mdl	-0.747	-0.724	-0.683	-0.699	-0.254
das2d3pc	0.070	0.069	-0.005	0.002	0.033
aps1	-0.451	-0.461	-0.361	-0.405	-0.184
scoma1	-0.309	-0.307	-0.082	-0.073	0.184
meanbp1	0.288	0.286	-0.057	-0.064	0.109
wblc1	0.093	0.099	0.013	0.007	0.031
hrt1	0.042	0.040	0.076	0.081	-0.016
resp1	-0.172	-0.166	-0.327	-0.310	-0.078
temp1	-0.180	-0.204	-0.108	-0.111	-0.051
alb1	-0.032	-0.040	0.064	0.061	0.033
bili1	0.022	0.022	0.007	0.008	0.015
crea1	0.081	0.093	0.001	0.013	0.012
sod1	0.051	0.035	0.010	0.008	-0.015
pot1	-0.209	-0.221	-0.130	-0.130	-0.055
wtkilo1	-0.059	-0.046	0.091	0.083	-0.028
dnr1	1.294	1.315	-0.117	-0.131	-0.062
resp	0.543	0.508	0.083	0.076	0.027
card	-0.037	-0.049	0.131	0.131	-0.045
neuro	0.570	0.588	-0.156	-0.191	0.126
gastr	-0.147	-0.144	-0.052	-0.022	-0.038
renal	-0.403	-0.414	-0.135	-0.167	-0.098
meta	-0.122	-0.100	-0.389	-0.391	-0.100
hema	0.733	0.786	-0.278	-0.275	0.003
seps	0.139	0.138	-0.185	-0.210	0.002
trauma	0.622	0.533	0.862	0.925	0.020
ortho	-0.353	-0.349	0.187	0.275	0.000
cat2_mosfs	-0.160	-0.140	0.588	0.604	0.042

cat2_coma	2.059	2.009	0.261	0.248	0.092
cat2_mosfm	1.363	1.360	0.586	0.674	0.108
cat2_lung	1.412	1.072	0.960	1.131	0.033
cat2_cirrh	2.134	2.101	0.047	0.061	0.007
cat2_colon	-0.005	-0.013	-0.239	-0.223	-0.028
ca_yes	0.355	0.182	-0.458	-0.498	-0.018
ca_meta	-0.053	-0.205	-0.608	-0.698	0.004
cat1_copd	0.155	-0.013	-0.320	-0.374	-0.006
cat1_mosfs	-0.017	-0.007	0.254	0.284	-0.084
cat1_mosfm	0.586	0.568	-0.447	-0.355	-0.112
cat1_chf	0.544	0.525	0.757	0.731	-0.005
cat1_coma	2.183	2.210	-0.091	-0.112	0.215
cat1_cirrh	0.398	0.386	-0.468	-0.399	-0.008
cat1_lung	1.740	1.711	-0.025	-0.098	0.062
cat1_colon	-0.129	-0.138	-0.171	-0.176	-0.013
ins_care	-0.255	-0.236	-0.439	-0.421	-0.097
ins_pcare	-0.242	-0.224	-0.391	-0.359	-0.085
ins_caid	-0.242	-0.252	-0.247	-0.229	-0.021
ins_no	0.647	0.644	-0.127	-0.111	-0.043
ins_carecaid	0.036	0.006	0.048	0.028	0.041
income1	-0.078	-0.089	0.094	0.110	0.061
income2	-0.246	-0.234	0.194	0.238	0.093
income3	-0.442	-0.390	0.224	0.251	0.072
raceblack	-0.018	0.009	0.192	0.226	0.051
raceother	0.206	0.251	0.292	0.277	0.130
wtki	-0.526	-0.518	0.586	0.546	0.125
pafil	-	-0.011	-	-	-
paco21	-	0.090	-	-	-
ph1	-	-	0.037	-	-
hema1	-	-	-0.061	-	-

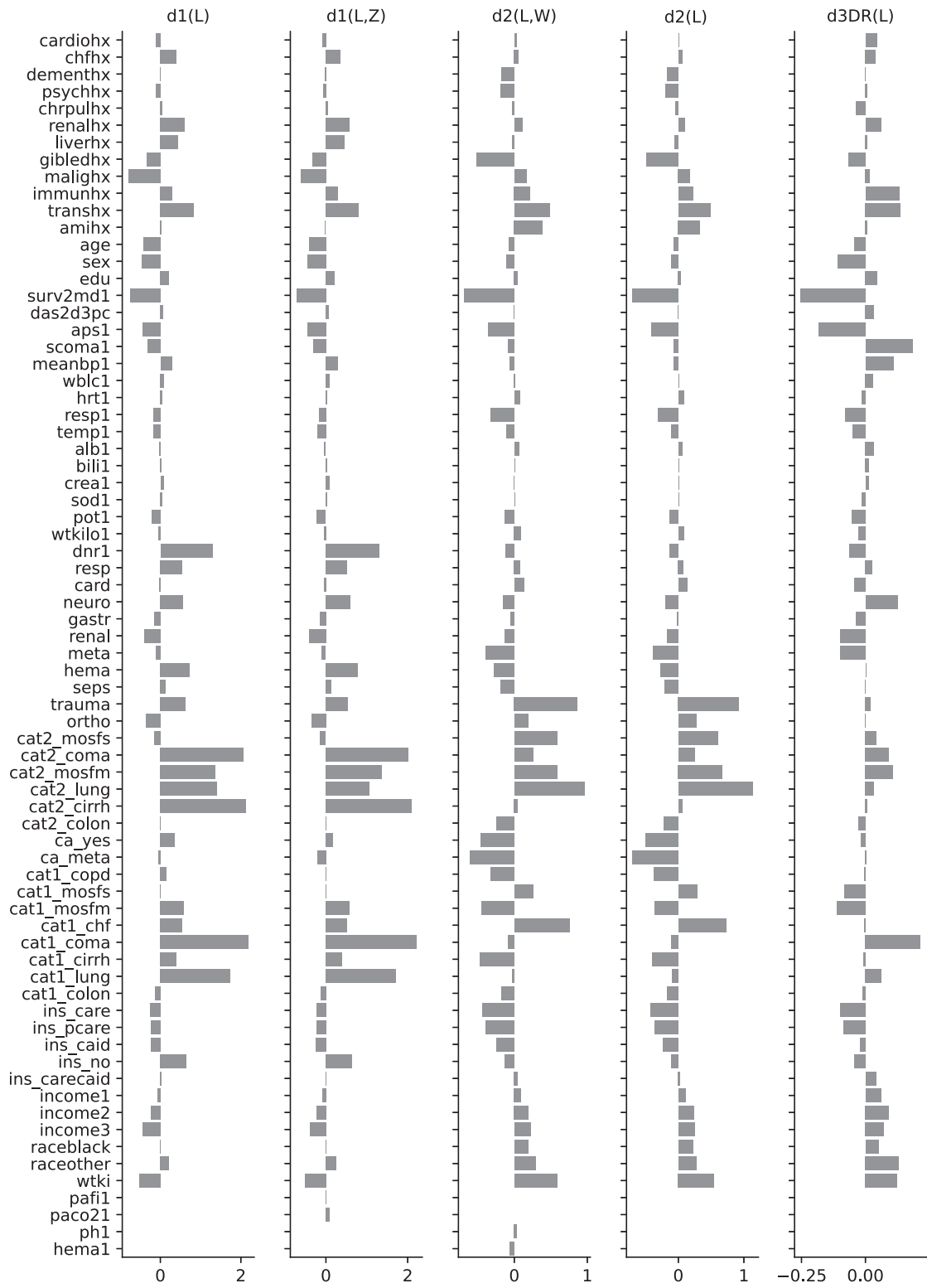


Figure 11: Sizes of all coefficients of the five optimal linear ITR estimates.

